

MONITORING LAND SURFACE DEFORMATION USING PERSISTENT  
SCATTERERS INTERFEROMETRIC SYNTHETIC APERTURE RADAR  
TECHNIQUE

NASUHA BINTI ISHAK

UNIVERSITI TEKNOLOGI MALAYSIA

MONITORING LAND SURFACE DEFORMATION USING PERSISTENT  
SCATTERERS INTERFEROMETRIC SYNTHETIC APERTURE RADAR  
TECHNIQUE

NASUHA BINTI ISHAK

A thesis submitted in fulfilment of the  
requirements for the award of the degree of  
Master of Science (Remote Sensing)

Faculty of Geoinformation and Real Estate  
Universiti Teknologi Malaysia

FEBRUARY 2017

In the name of Allah, Most Gracious Most Merciful

All praise and thanks are due to Allah Almighty and  
peace and blessing be upon His Messenger

*This thesis is dedicated to my parents*

*For their endless love, support and encouragement*

## ACKNOWLEDGEMENT

First and foremost, thanks to Allah SWT for giving me strength and opportunity to complete my master study. I am heartily thankful to my supervisor Dr. Md Latifur Rahman Sarker for his constant encouragement, supervision, supporting and guidance during my study. I believed I learned from the best and I am truly grateful for his guide. I would also like to convey my deepest gratitude to my co-supervisor, Dr. Ami Hassan bin Md Din who has helped me in many ways during all these times.

Deepest thanks and appreciation goes to my parents (Ishak bin Ali and Zouyah binti Majid) and my siblings for their endless love and prayers. To all my friends, thank you for your understanding and encouragement in moments of crisis. I have been blessed with a friendly, helpful and encouraging group of friends and labmates.

I would also like to acknowledge the Ministry of Higher Education Malaysia for the scholarship under MyMaster program and all financial research support including Ministry of Higher Education (MOHE) for providing grant (R.J130000.7827.4F689) entitled “Determination of Floodplain Change and its Impact on Flood Modelling Using Multi-Temporal DEM and Land Use/Land Cover from InSAR/SAR Technique”. Special thanks also goes to Japan Aerospace Exploration Agency (JAXA) for providing the ALOS data, under the project No. P1387002. Lastly, I offer my regards and blessings to all of those who supported me in any respect during the completion of this study.

## ABSTRACT

Land subsidence is one of the major hazards occurring globally due to several reasons including natural and human activities. The effect of land subsidence depends on the extent and severity. The consequences of this hazard can be seen in many forms including damaged of infrastructures and loss of human lives. Although land subsidence is a global problem, but it is very common in urban and sub urban areas especially in rapidly developing countries. This problem needs to be monitored effectively. Several techniques such as land surveying, aerial photogrammetry and Global Positioning System (GPS) can be used to monitor or detect the subsidence effectively but these techniques are mostly expensive and time consuming especially for large area. In recent decades, Interferometric Synthetic Aperture Radar (InSAR) technique has been used widely for the monitoring of land subsidence successfully although this technique has several limitations due to temporal decorrelation, atmospheric effects and so on. However, the uncertainties related to InSAR technique have been reduced significantly with the recent Persistent Scatterers Interferometric Synthetic Aperture Radar (PSInSAR) technique which utilized a stack of interferograms generated from several radar images to estimate deformation by finding a bunch of stable points. This study investigates the surface deformation focusing on Kuala Lumpur, a rapidly growing city and Selangor using PSInSAR technique with a set of ALOS PALSAR images from 2007 to 2011. The research methodology consists of several steps of image processing that includes i) generation of Differential Interferometric Synthetic Aperture Radar (DInSAR), ii) selection of Persistent Scatterers (PS) points, iii) removal of noise, iv) optimization of PS point selection, and v) generation of time series deformation map. However, special consideration was given to optimize the PS selection process using two master images. Results indicate a complete variation of mean line-of-sight (LOS) velocities over the study area. Stable areas (mean LOS=1.1 mm/year) were mostly found in the urban center of Kuala Lumpur, while medium rate of LOS (from 20 mm/year to 30 mm/year) was observed in the south west area in Kuala Langat and Sepang districts. The infrastructures in Kuala Lumpur are mostly stable except in Kuala Lumpur International Airport (KLIA) where a significant subsidence was detected (28.7 mm/year). Meanwhile, other parts of the study area such as Hulu Langat, Petaling Jaya and Klang districts show a very low and non-continuous movement (LOS < 20 mm/year), although comparatively higher subsidence rate (28 mm/year) was detected in the mining area. As conclusion, PSInSAR technique has a potential to monitor subsidence in urban and sub urban areas, but optimization of PS selection processing is necessary in order to reduce the noise and get better estimation accuracy.

## ABSTRAK

Pemendapan tanah merupakan salah satu bahaya utama yang berlaku di peringkat global kerana beberapa sebab merangkumi aktiviti semula jadi dan aktiviti manusia. Kesan pemendapan tanah bergantung kepada tahap dan keterukan. Kesan bahaya ini dapat dilihat dalam pelbagai bentuk termasuk kerosakan infrastruktur dan kehilangan nyawa manusia. Walaupun pemendapan tanah adalah masalah global, namun ia merupakan perkara biasa di kawasan bandar dan sub bandar terutamanya di negara-negara pesat membangun. Masalah ini perlu dipantau dengan berkesan. Beberapa teknik seperti ukur tanah, fotogrametri udara dan sistem kedudukan global (GPS) boleh digunakan untuk memantau atau mengesan pemendapan dengan berkesan tetapi teknik-teknik ini kebanyakannya mahal dan mengambil masa terutamanya bagi kawasan yang besar. Dalam dekad kebelakangan ini, teknik radar apertur sintetik interferometer (InSAR) telah digunakan secara meluas untuk memantau pemendapan tanah dengan jayanya walaupun teknik ini mempunyai beberapa batasan kerana nyahkolerasi masa, kesan atmosfera dan sebagainya. Walau bagaimanapun, ketidaktentuan yang berkaitan dengan teknik InSAR telah dikurangkan baru-baru ini dengan ketara dengan teknik radar apertur sintetik interferometer penyerak berterusan (PSInSAR) yang menggunakan timbunan interferogram dijana daripada beberapa imej radar untuk menganggar deformasi dengan mencari sekumpulan titik stabil. Kajian ini mengkaji deformasi permukaan dengan memberi tumpuan kepada Kuala Lumpur, bandar yang berkembang pesat dan Selangor menggunakan teknik PSInSAR dengan satu set imej ALOS Palsar dari 2007 hingga 2011. Metodologi kajian terdiri daripada beberapa langkah pemrosesan imej merangkumi i) penjanaan radar apertur sintetik interferometer berbeza (DInSAR), ii) pemilihan titik penyerak berterusan (PS), iii) penyingkiran gangguan, iv) pengoptimuman pemilihan titik PS, dan v) penerbitan peta deformasi siri masa. Walau bagaimanapun, pertimbangan khas telah diberikan untuk mengoptimumkan proses pemilihan PS menggunakan dua imej induk. Keputusan menunjukkan pelbagai variasi halaju min garis penglihatan (LOS) bagi kawasan kajian. Kawasan stabil (min LOS = 1.1 mm / tahun) didapati tertumpu di pusat bandar Kuala Lumpur, manakala kadar sederhana LOS (dari 20 mm/tahun sehingga 30 mm/tahun) dilihat di kawasan barat daya di daerah Kuala Langat dan Sepang. Infrastruktur di Kuala Lumpur kebanyakannya stabil kecuali di Lapangan Terbang Antarabangsa Kuala Lumpur (KLIA) di mana penenggelaman yang ketara telah dikesan (28.7 mm/tahun). Sementara itu, bahagian lain kawasan kajian seperti daerah Hulu Langat, Petaling Jaya dan Klang menunjukkan pergerakan yang sangat rendah dan tidak berterusan (LOS <20 mm/tahun), walaupun kadar penenggelaman yang agak tinggi (28 mm/tahun) telah dikesan di kawasan perlombongan. Kesimpulannya, teknik PSInSAR mempunyai potensi untuk memantau pemendapan di kawasan bandar dan sub bandar, tetapi proses mengoptimumkan pemilihan PS adalah perlu untuk mengurangkan gangguan dan mendapatkan anggaran ketepatan yang lebih baik.

## TABLE OF CONTENTS

<b>CHAPTER</b>	<b>TITLE</b>	<b>PAGE</b>
	<b>DECLARATION</b>	ii
	<b>DEDICATION</b>	iii
	<b>ACKNOWLEDGEMENTS</b>	iv
	<b>ABSTRACT</b>	v
	<b>ABSTRAK</b>	vi
	<b>CONTENTS</b>	vii
	<b>LIST OF TABLES</b>	xii
	<b>LIST OF FIGURES</b>	xiv
	<b>LIST OF SYMBOLS</b>	xxiii
	<b>LIST OF ABBREVIATIONS</b>	xxvi
	<b>LIST OF APPENDICES</b>	xxxix
<b>1</b>	<b>INTRODUCTION</b>	<b>1</b>
	1.1 Background of Research	1
	1.2 Problem Statement	7
	1.3 Research Objectives	11
	1.4 Study Area	12
	1.5 Scope of Study	14
	1.6 Significance of Study	15
	1.7 Outline of Thesis	16

<b>2</b>	<b>LITERATURE REVIEW</b>	<b>19</b>
2.1	Radar	19
2.2	Synthetic Aperture Radar	20
2.2.1	Basic Principles of Synthetic Aperture Radar	21
2.2.2	Image Properties	22
2.2.2.1	Amplitude Image	23
2.2.2.2	The Phase SAR image	24
2.2.2.3	Factors Affecting the Phase of an Image Pixel	26
2.3	Interferometric Synthetic Aperture Radar	27
2.3.1	Interferogram	29
2.3.2	Coherence	33
2.3.3	General Processing of Interferometric Synthetic Aperture Radar	34
2.3.3.1	Co-Registration	35
2.3.3.2	Phase Unwrapping	38
2.4	Phase Contribution in Interferogram	43
2.5	Differential Interferometric Synthetic Aperture Radar	44
2.5.1	Interferogram Flattening	44
2.5.2	Topography Removal	45
2.6	Other Errors Associated with the Differential Interferogram	48
2.6.1	Decorrelation	48
2.6.6.1	Thermal Decorrelation	49
2.6.6.2	Geometrical Decorrelation	50
2.6.6.3	Doppler Centroid Decorrelation	50
2.6.6.4	Processing Decorrelation	51
2.6.6.5	Temporal Decorrelation	51
2.6.2	Atmospheric Effects	51
2.7	Time-series Interferograms	54

2.8	Persistent Scatterers Interferometric Aperture Radar	56
<b>3</b>	<b>METHODOLOGY</b>	<b>60</b>
3.1	Introduction	61
3.2	Data Preparation and Software Selection	62
3.2.1	Sensor and Image Catalogue	62
3.2.2	Data Availability and Selection	64
3.2.3	Software Tools	65
3.2.4	SAR Data Focusing	67
3.3	Differential Interferogram Processing	69
3.3.1	Multi-looking	69
3.3.2	Master Image Selection	71
3.3.3	Co-Registration	74
3.3.3.1	Coarse Co-Registration	74
3.3.3.2	Fine Co-Registration	76
3.3.4	Raw Interferogram Generation	78
3.3.5	Coherence Image Generation	80
3.3.6	Differential Interferogram Computation	81
3.3.6.1	Interferogram Flattening	82
3.3.6.2	Reference DEM subtraction	84
3.3.7	Geocoding	85
3.4	Persistent Scatterers Interferometric Aperture Radar Methodology	86
3.4.1	Phase Stability Estimation	86
3.4.1.1	Initial PS Candidate Selection	87
3.4.1.2	Phase Noise Estimation	87
3.4.2	PS Final Selection	88
3.4.2.1	PS Selection	88
3.4.2.2	PS Weeding	89
3.4.2.3	PS Correction	90
3.4.3	Displacement Estimation	92

	3.4.3.1 Phase Unwrapping	93
	3.4.3.2 Estimating Spatially Correlated Errors	94
	3.4.3.3 Filtering Other Spatially Correlated Noise.	95
<b>4</b>	<b>RESULTS AND DISCUSSION</b>	<b>100</b>
	4.1 Introduction	100
	4.2 Preliminary Results	101
	4.3 Optimization of PSInSAR processing parameters	105
	4.3.1 Maximum Acceptable Spatial Density of Selected Pixels with Random Phase	107
	4.3.2 Maximum Standard Deviation of the Phase Noise	108
	4.3.3 Threshold of Maximum Standard Deviation of 0.8 and 0.5 radian	109
	4.3.3.1 Spatially Correlated Filtering Time Window.	112
	4.3.3.2 Unwrapping Grid Cell Size.	114
	4.3.3.3 Coarser Resample Size.	117
	4.3.3.4 Maximum Standard Deviation of The Resampled Pixels of Phase Noise	120
	4.4 Comparison Results and Discussion	122
	4.5 Final Results and Discussion	126
	4.6 Time-Series and Field Inspection	130
	4.6.1 Kuala Lumpur	130
	4.6.2 Hulu Langat	134
	4.6.3 Petaling Jaya	136
	4.6.4 Putrajaya	142
	4.6.5 Sepang	144

4.6.6	Kuala Langat	147
4.6.7	Gombak	151
4.6.8	Hulu Selangor	152
4.6.9	Klang	155
4.6.10	Kuala Selangor	157
<b>5</b>	<b>DISCUSSIONS</b>	<b>161</b>
<b>6</b>	<b>CONCLUSIONS AND RECOMMENDATIONS</b>	<b>169</b>
6.1	Introduction	169
6.2	Conclusion	169
6.3	Recommendations	172
	<b>REFERENCES</b>	<b>173</b>
	Appendices A-H	206-221

## LIST OF TABLES

TABLES NO	TITLE	PAGE
3.1	Ascending orbit data for study areas (track 151) acquired by ALOS PALSAR. Doppler centroid, temporal baselines and perpendicular baselines relative to master acquisition on 2009-07-03	64
3.2	Estimated rho values for each dataset	73
3.3	Line and Pixel offsets of slave images after coarse co-registration	75
3.4	The change in mean value of $\gamma$ until it converged at 0.005 value	88
4.1	Initial parameters used in the PSInSAR processing of Kuala Lumpur	101
4.2	Maximum acceptable noise density and corresponding PS candidates in six patches	107

- 4.3 Detected PS points using spatially correlated filtering time window parameter thresholds of 730 days, 300 days and 180 days and weed standard deviation of 0.8 and 0.5 in both master images 112
- 4.4 Detected PS points using unwrapping grid cell size parameter thresholds of 200 m and 100 m and weed standard deviation of 0.8 and 0.5 in both master images 115
- 4.5 Detected PS points using coarser resampling size parameter thresholds of 200 m, 100 m and 50 m and weed standard deviation of 0.8 and 0.5 in both master images 117
- 4.6 Detected PS points using maximum standard deviation of the resampled pixels of phase noise parameter thresholds of three 0.8 radian, 0.6 radian and 0.2 radian and weed standard deviation of 0.8 and 0.5 in both master images 120

## LIST OF FIGURES

FIGURE NO	TITLE	PAGE
1.1	Location of Kuala Lumpur, Selangor.	13
2.1	Acquisition geometry of SAR system (Bennett and Blacknell, 2003).	21
2.2	The relationship among amplitude, phase, and wavelength of a radar signal. The intensity of the radar signal is proportional to the squared amplitude. (Zhou <i>et al.</i> , 2009)	23
2.3	Amplitude of an SLC image (Milan, Italy acquired by ERS SAR). Strong reflectors are visualized in white whereas areas with limited reflection towards the satellite are represented in black) (ESA, 2007)	24
2.4	A sinusoidal function $\sin \varphi$ is periodic with a $2\pi$ radian period (ESA, 2007).	25
2.5	A schematic showing the relationship between ground displacement and signal phase shift during first and second acquisition of SAR images on the same area. The numerical value of the wavelength is ERS wavelength which is 5.66 cm (Jha <i>et al.</i> , 2015)	28

- 2.6 (a) Phase of an SLC image. Only the fractional phase of the received signal is recorded, resulting in phase values between  $-\pi$  and  $+\pi$ . The phase in an SLC image cannot be interpreted directly. (b) Phase of an interferogram. After combination of two SLC images, interpretable phase information is obtained (Yun *et al.*, 2007) 30
- 2.7 An interferogram generated from two radar images. Acquisition were taken before the L'Aquila Earthquake (February 2009) and after event (April 2009). The fringes indicate coherence whereby displacement can be calculated in the corresponding areas. The areas with a spotty appearance are areas where decorrelation noise has occurred. Phase values ranges from  $-\pi$  to  $+\pi$  (ESA, 2007). 31
- 2.8 ERS-2 SAR detected image of the Linate Airport in the eastern part of Milan (Italy): the speckle effect on the homogeneous fields surrounding the airport is clearly visible (ESA, 2007). 32
- 2.9 TANDEM-X (a) interferogram and (b) coherence image over the Franz Josef Land, Russia (Villano and Kreiger, 2012). 34
- 2.10 General procedures of fine co-registration (Liao *et al.*, 2004) 36
- 2.11 (a) Wrapped interferogram in radian and (b) unwrapped phase of the same interferogram in centimetre at Longonot volcano, Kenyan Rift. (Robertson *et al.*, 2015). 39
- 2.12 A comparison of the unwrapped and wrapped signal in 1 dimensional (1-D). Black solid line is the continuous unwrapped solution, and red dashed line is the wrapped version (Li *et al.*, 2007) 40
- 2.13 a) Raw interferogram, b) flat-earth contribution calculated from orbit information and c) flattened interferogram after flat earth removal (Frey *et al.*, 2013). 45

2.14	a) Raw interferogram with some visible close fringes, b) differential interferogram with topography contribution removed covering the entire Austfonna, Svalbard (Moholdt and Kaab, 2012).	46
2.15	Noise found in the centre of the interferograms during Wenchuan earthquake, China (Tong <i>et. al.</i> , 2010).	49
2.16	Interferogram for Tucson region covering the period Jan 27 to April 6, 1996, from Hoffmann (2003). There was no appreciable deformation during this time period and all the phase variation seen here is due to variation in atmospheric path delay during repeat-pass observation. The image is approximately 50 x 50 km, and each color fringe represents 2.8 cm of relative path delay.	53
2.17	Phase simulations for (a) a distributed scatterer pixel and (b) a persistent scatterer pixel (Piyush, 2010).	56
3.1	Overall methodology	61
3.2	Japan Aerospace Exploration Agency (JAXA) website for ALOS data ordering.	63
3.3	SAR Data Focusing Process	67
3.4	(a) Intensity image (b) Phase image (c) Intensity image overlaid with Phase image on 03 July 2009	68
3.5	The amplitude of SLC image dated on 03 July 2009 with (a) Non-Multilooking and (b) Multilook image (2 azimuth looks and 1 range looks)	69
3.6	Offsets between Master image (1997-10-18) and Slave image (1996-04-06) where (a) observed offsets and (b) estimated model vectors	76

3.7	Absolute errors between model and observations in azimuth and range (a) residuals and (b) standard deviations of residuals	77
3.8	Raw interferograms	79
3.9	Coherence image between 10 February 2007 and master image (03 July 2009).	82
3.10	Interferograms after phase subtraction	83
3.11	Interferograms after phase and topography subtraction	85
3.12	Wrapped phases of final selected persistent scatters	91
3.13	Initial unwrapped phases of selected persistent scatters.	93
3.14	Phases due to orbital ramp errors in radian	94
3.15	Phase due to spatially correlated look angle error in radian/meter	95
3.16	Atmospheric Phase Screen due to master atmosphere and orbit error	95
3.17	Unwrapped phases after subtraction of spatially correlated look angle error from initial unwrapped phase	96
3.18	Results of atmospheric phase screen due to slave atmosphere and orbit error	97
3.19	New unwrapped phases after subtraction of spatially correlated look angle error, Atmospheric Phase Screen due to master and slave atmosphere, orbit error and orbital ramp from initial unwrapped phase	98

4.1	Wrapped PS interferograms acquired in the study area overlaid with SRTM shaded relief. The master acquisition date is 03 July 2009. Each colour fringe represents 12.1 cm of displacement in the line-of-sight.	102
4.2	Initial deformation map from ALOS PALSAR superimposed on a mean amplitude image.	103
4.3	Flow diagram of PS optimization process	106
4.4	Wrapped PS interferogram on 21 August 2010, a) using weeding standard deviation of 1.2, b) using weeding standard deviation of 1.0, c) using weeding standard deviation of 0.8, d) using weeding standard deviation of 0.5, and e) using weeding standard deviation of 0.2. Phase values ranges from $-\pi$ to $+\pi$	110
4.5	The mean velocity in line-of-sight for spatially correlated filtering time window thresholds of i) 730 days, ii) 300 days and iii) 180 days and weed standard deviation of 0.8 for both master images	113
4.6	The mean velocity in line-of-sight for spatially correlated filtering time window thresholds of i) 730 days, ii) 300 days and iii) 180 days and weed standard deviation of 0.5 for both master images	113
4.7	The mean velocity in line-of-sight for unwrapping grid cell size parameter thresholds of i) 200 m and ii) 100 m and weed standard deviation of 0.8 for both master images.	116
4.8	The mean velocity in line-of-sight for unwrapping grid cell size parameter thresholds of i) 200 m and ii) 100 m and weed standard deviation of 0.5 for both master images.	116

- 4.9 The mean velocity in line-of-sight for coarser resample size parameter thresholds of i) 200 m, ii) 100 m and iii) 50 m and weed standard deviation of 0.8 for both master images. 118
- 4.10 The mean velocity in line-of-sight for coarser resample size parameter thresholds of i) 200 m, ii) 100 m and iii) 50 m and weed standard deviation of 0.5 for both master images. 118
- 4.11 A close view of PS pixels superimposed on a mean amplitude image using (a) 200 m and (b) 50 m where more PS discontinuities were found in (a) 119
- 4.12 The mean velocity in line-of-sight for maximum standard deviation of noise parameter thresholds of i) 0.8 radian, ii) 0.6 radian and iii) 0.2 radian and weed standard deviation of 0.8 for both master images. 121
- 4.13 The mean velocity in line-of-sight for maximum standard deviation of noise parameter thresholds of i) 0.8 radian, ii) 0.6 radian and iii) 0.2 radian and weed standard deviation of 0.5 for both master images. 121
- 4.14 Mean velocity in line-of-sight on the centre of Kuala Lumpur (a) default settings, (b) optimized parameter using master image July 2009 and (c) optimized parameter using master image February 2007. The red dashed circles show the random pixels found in the area which later disappeared after optimization of parameters in (b) and (c). 123
- 4.15 Mean velocity in line-of-sight (a) default settings, (b) optimized parameter using master image July 2009 and (c) optimized parameter using master image February 2007 125

- 4.16 Cumulative LOS displacement plotted on shaded relief SRTM topography where the red box refers to the city centre of the study area. 126
- 4.17 Mean LOS velocities in Kuala Lumpur and neighbouring areas plotted on shaded relief SRTM topography where orange line refers to the boundary between study area and other states. 127
- 4.18 Standard Deviation of Mean LOS velocity plotted on shaded relief SRTM topography where blue line refers to the boundary between study area and other states. Two red boxes denoted with A and B indicate the places with highest standard deviation. 129
- 4.19 A close up view on the highest standard deviation of mean LOS velocity on shaded relief SRTM topography which is located in high relief area. 129
- 4.20 Selected PS points for time analysis in Kuala Lumpur area. 131
- 4.21 Displacement time series during 2007-2011 of the selected PS points a) P1, b) P2, and c) P3 in Figure 4.20. 132
- 4.22 Selected PS point for time analysis in Batu Caves area. 133
- 4.23 Displacement time series during 2007-2011 of the selected PS point (P4) in Figure 4.22. 134
- 4.24 Selected PS point for time analysis near Pandan Indah town in Hulu Langat district 135
- 4.25 Displacement time series during 2007-2011 of the selected PS point (P5) in Figure 4.24. 135

4.26	Selected PS point for time analysis in the Bukit Lanjan area	136
4.27	Selected PS point for time analysis in the Bukit Damansara area	137
4.28	Displacement time series during 2007-2011 of the selected PS points a) P6 in Figure 4.26 and b) P7 in Figure 4.27	137
4.29	Selected PS points for time analysis in the Subang Airport area.	138
4.30	Displacement time series during 2007-2011 of the selected PS points a) P8 and b) P9 in Figure 4.29	139
4.31	Selected PS points for time analysis in Petaling Jaya district.	140
4.32	Displacement time series during 2007-2011 of the selected PS points a) P10 and b) P11 in Figure 4.31.	141
4.33	The PS points distribution in the Putrajaya area	142
4.34	A close view on PS distribution and selected PS point for time analysis in the Precinct 5, Putrajaya area.	143
4.35	Displacement time series during 2007-2011 of the selected PS point (P12) in Figure 4.34.	143
4.36	Selected PS points for time analysis in the Kuala Lumpur International Airport area	145
4.37	Displacement time series during 2007-2011 of the selected PS points a) P13 and b) P14 in Figure 4.36	146
4.38	The PS points distribution in Kuala Langat district where two distinct deformations patterns were found, 1) slow rate near Banting town and 2) medium rate near Morib beach.	147

4.39	Selected PS point for time analysis near Banting town northern of Kuala Langat district.	148
4.40	Displacement time series during 2007-2011 of the selected PS point (P15) in Figure 4.39	148
4.41	Langat basin is 78 km long with a catchment of 2350 km <sup>2</sup> which originates from the Titiwangsa Mountains and drains westward to the Straits of Malacca (Nurfashareena <i>et al.</i> , 2015).	149
4.42	Selected PS point for time analysis near Morib area at the southern of Kuala Langat district	150
4.43	Displacement time series during 2007-2011 of the selected PS point (P16) in Figure 4.42	150
4.44	Selected PS point for time analysis in Gombak area.	151
4.45	Displacement time series during 2007-2011 of the selected PS point (P17) in Figure 4.44.	152
4.46	Selected PS points for time analysis in Hulu Selangor district	153
4.47	Displacement time series during 2007-2011 of the selected PS points a) P18, b) P19 and c) P20 in Figure 4.46 respectively	154
4.48	The PS points distribution in Klang area	155
4.49	A close view on PS distribution and selected PS point for time analysis in Bandar Bukit Raja area.	156
4.50	Displacement time series during 2007-2011 of the selected PS point (P21) in Figure 4.49	156

4.51	The PS points distribution in Kuala Selangor district	157
4.52	A close view on PS distribution and selected PS points for time analysis in the mining area where located in Hulu Selangor	158
4.53	Displacement time series during 2007-2011 of the selected PS points a) P22 and b) P23 in Figure 4.52	159
4.54	Field evidences of active sand mining activities over the Bestari Jaya town where an arrow indicates subsiding deformation connected to the (a) water pond cliff (localized on P23 in Figure 4.52), (b) sand piles in the mining area (localized on P24 in Figure 4.52), while (c) and (d) are the observed water ponds associated with groundwater pumping activities in the mining area	160

## LIST OF SYMBOLS

$\phi$	Phase
$\mathbf{k}$	Complex wave vector
$\mathbf{R}$	Slant range
$t$	Time
$\omega$	Wave angular frequency
$\gamma$	Complex correlation coefficient
$E[]$	Complex conjugate
$\rho$	Coherence
$ \gamma $	Amplitude of the complex correlation coefficient
$f_{\text{DC}}$	Doppler centroid frequencies
$\Delta\varphi_{\text{total}}$	Total phase contribution
$\Delta\varphi_{\text{ref}}$	Phase related to flat-earth
$\Delta\varphi_{\text{topo}}$	Phase related to topography
$\Delta\varphi_{\text{atmo}}$	Phase related to atmosphere
$\Delta\varphi_{\text{deco}}$	Phase related to decorrelation
$\Delta\varphi_{\text{noise}}$	Phase related to Phase noise
$\Delta\varphi_{\text{defo}}$	Phase related to terrain deformation
$\Delta\varphi_{\text{ref}}$	Phase difference exists between two points
$\varphi_{\text{orb}}$	Phase due to the inaccurate orbits
$\pi$	Ratio of a circle's circumference to its diameter
$B_{\perp}$	Perpendicular baselines
$\Delta R$	Range distance difference
$\lambda$	Wavelength
$r$	Slant range coordinate

$\theta$	Elevation angle
$h$	Height
$\theta_{inc}$	Incidence angle
$\gamma_{total}$	Sources of decorrelation effects
$\gamma_{therm}$	Thermal decorrelation
$\gamma_{geom}$	Geometrical decorrelation
$\gamma_{DC}$	Doppler centroid decorrelation
$\gamma_{proc}$	Processing decorrelation
$\gamma_{temp}$	Temporal decorrelation
$\rho_{total}$	Total correlation
$\rho_{temporal}$	Temporal correlation
$\rho_{spatial}$	Spatial correlation
$\rho_{dopler}$	Correlation in Doppler centroid frequency
$\rho_{thermal}$	Correlation in thermal noise
$T$	Temporal baseline
$T^c$	Phase related to atmosphere
$B_{\perp}^c$	Critical perpendicular baselines
$F_{DC}$	Doppler centroid frequency
$F_{DC}^c$	Critical Doppler centroid frequency
$f(x)$	Phase difference exists between two points
$f$	Phase due to the inaccurate orbits
$i$	Imaginary band
$p$	Power
$r$	Real band
$I$	Complex interferogram
$M$	Complex master image
$S$	Complex resampled slave image
$\emptyset_I$	Observed phase difference
$\emptyset_M$	Phase due to master image
$\emptyset_S$	Phase due to slave image
$\gamma_c$	Complex coherence
$E\{.\}$	The expectation
$N$	Number of images

$R$	Complex reference phase
$D_a$	Amplitude dispersion index
$\mu_a$	Mean of the amplitudes
$\sigma_a$	Standard deviation the amplitudes
$\sigma_\emptyset$	PS candidates
$\gamma$	Coherence-like measure

## LIST OF ABBREVIATION

1D	1 dimensional
2D	2 dimensional
3D	3 dimensional
ALOS	Advanced Land Observing Satellite
AOE	Atmospheric and orbit error
ASAR	Advanced Synthetic Aperture Radar
ASTER	Advanced Spaceborne Thermal Emission and Reflection Radiometer
AVINIR	Advanced Visible and Near Infrared Radiometer
CalTech	California Institute of Technology
cm	Centimetre
COSMO-SkyMed	Constellation of Small Satellites for Mediterranean basin Observation
DCT	Discrete cosine transform
DePSI	Delft Persistent Scatter Interferometry
DEM	Digital elevation model
DInSAR	Differential Interferometric Synthetic Aperture Radar
DORIS	Delft object-oriented radar interferometric software
EDM	Electronic distance metres
ENVISAT	Environmental Satellite
ERS	European remote sensing satellite
ESA	European Space Agency
FBS	Fine Beam Single Polarisation
FBD	Fine Beam Double Polarisation
FFT	Fast Fourier Transform

GDEM	Global Digital Elevation Map
GIMP	GNU Image Manipulation Program
GUI	Graphical User Interface
GPS	Global Positioning System
InSAR	Interferometric Synthetic Aperture Radar
JAXA	Japan Aerospace Exploration Agency
KLCC	Petronas Twin Towers
KLIA	Kuala Lumpur International Airport
Km	Kilometer
LOS	Line-of-sight
MERIS	Medium Resolution Imaging Spectrometer
MLV	Mean Line of Sight velocity
m	Meter
mm	Millimetre
MODIS	Moderate Resolution Imaging Spectroradiometer
NASA	National Aeronautics and Space Administration
PALSAR	Phased Array type L-band Synthetic Aperture Radar
PRC	Precise orbital data
PRISM	Panchromatic Remote-sensing Instrument for Stereo Mapping
PS	Persistent Scatterer
PSInSAR	Persistent Scatterer Interferometric Synthetic Aperture Radar
rad	Radian
Radar	Radio Detection and Ranging
ROI PAC	Repeat Orbit Interferometry Package
SAR	Synthetic Aperture Radar
SBAS	Small Baseline Subset
SCLA	Spatially correlated look angle
SLC	Single Look Complex
SNR	Signal-to-noise ratio
SRTM	Shuttle Radar Topography Mission
StaMPS	Stanford Method for Permanent Scatterers
SUBANG	Sultan Abdul Aziz Shah Airport
TerraSAR-X	German synthetic aperture radar Earth observation satellite
TU Delft	Delft University of Technology

viStaMPS	Visual Stanford Method for Permanent Scatterers
WGS84	World Geodetic System 1984
WRF	Weather Research and Forecast
yr	Year

**LIST OF APPENDICES**

<b>APPENDIX</b>	<b>TITLE</b>	<b>PAGE</b>
A	Wrapped interferograms	205
B	Unwrapped interferograms	208
C	DEM Uncertainty Error	211
D	Atmospheric Phase Contribution for Master	212
E	Atmospheric Phase Contribution for Slaves	213
F	Phase Ramps Error	215
G	Unwrapped Interferograms after Subtracting All Errors	217
H	Coastal Erosion along the Selangor Coast	220

## **CHAPTER 1**

### **INTRODUCTION**

This chapter consists of several sections including research background, problem statement, objectives, study area, significance, scopes and outlines of the thesis. The aim of this study is determined after doing an extensive background study related to this research in order to develop the best model for land surface deformation monitoring using PSInSAR technique.

#### **1.1 Background of Research**

Ground movement is the change of shapes of the ground surface induced by natural or human-phenomenon internally or externally (Qiao *et al.*, 2011; Jensen and Cowen, 1999), which happens very slowly yet may have sudden and far-reaching effects that endanger infrastructures or even human lives (Liu *et al.*, 2008). Apparently, the topographic changes in one particular area can create and destroy the surface features surrounding the ground which can eventually impose some active deformation onto nearby structures as well as below the ground such as pipe lines

and tunnels (Fornaro *et al.*, 2009). In general, the damage due to the ground movement can be attributed by several factors such as shrinkage of soils, landslip, ground water extraction, mine collapse, settlement of land reclamation sites and poor/faulty construction of big infrastructures (Yoo and Lee, 2008; Akcin *et al.*, 2010). However, deep excavation projects for high-rise buildings and subways are also the important factors for land surface deformation in the urban and sub-urban areas (Jensen and Cowen, 1999; Yoo and Lee, 2008).

The extensive as well as rapid infrastructure development in urban and sub-urban areas plays an important role in occurring the land subsidence around the world as various infrastructures in urban areas are most likely to subside due to several reasons especially the inability of the land to accommodate the pressure from the big infrastructures (Jensen and Cowen, 1999; Berardino *et al.*, 2002), the rapid conversion of natural properties (such as forest and agricultural land) into developed land (Berardino *et al.*, 2002), and over-extraction of ground water exploitation for domestic and industrial purposes (Sahu and Sikdar, 2011; Gupta and Srivastava, 2010). Additionally, studies found that there is an impact of natural hazards and anthropogenic activities on land subsidence. For example, remarkable engineered structures such as Taipei 101, the world's tallest building (Liu *et al.*, 2001), Chek Lap Kok airport in Hong Kong (Lin, 2005) and Conza Dam in the southern Apennines, Italy (Martire *et al.*, 2014) were detected sensitive to force triggered not only by natural hazards but also human activities resulting the damage of infrastructures with cracking and sinkhole.

Indeed, land subsidence/deformation is global problem and monitoring this problem using an effective technology is essential especially in urban areas and sub-urban areas to ease the rising public concern on the effects of construction-induced as well as underground water exploitation movements to the environments (Ferronato *et al.*, 2006; Worawattanamateekul *et al.*, 2003). However, this monitoring/warning system should be in a long time acquisition resulting from continuous monitoring instrumentation to monitor different types of terrain deformation phenomena such as subsidence, landslides, seismic activity and underground deformation despite the

difficulties in operational conditions such as in remote areas and during heavy rainfall (Velez *et al.*, 2011; Wallace *et al.*, 2012).

In the past, monitoring surface deformation has been conducted using a variety of surveying techniques to track movements on the unstable areas (Wilson and Mikkelsen, 1978). Theodolite, electronic distance metres (EDM) and total station measurements give the point coordinates and changes of target and hence allow the detection of landslides features (Ashkenazi *et al.*, 1980). Tapes and wire devices have been used to measure changes in distance of crack walls (Gulla *et al.*, 1988). These ground surface movement measurement techniques are widely used but known to be time consuming and usually require large man power to complete the survey over a large area (Bonforte *et al.*, 2001). Aerial or terrestrial photogrammetry provides the point coordinates, contour maps and the cross-sections of the landslides with typical precision of 20 cm, however the process of acquiring aerial photograph is very expensive (Mikkelsen, 1996). Later, the Global Positioning System (GPS) is becoming progressively useful for monitoring deformation with the establishment of ground station. Several available GPS receivers have been used to detect the landslides features in the Swiss Alps and the precision obtained was about 1 cm (Bonnard *et al.*, 1996). However, the ground-based surface monitoring technique like GPS networks are often found less efficient in large areas and barely accessible in remote areas (Noferini *et al.*, 2005). In addition, the availability of GPS stations in the area of interest is often poor; leading to strongly extrapolated data modelling (Lauknes *et al.*, 2011).

The exploitation of Interferometric Synthetic Aperture Radar (InSAR) technique in the monitoring earth surface has started over the past few years and seems to be a great tool for rapid detecting surface change. This remote sensing technique is continuous and capable to monitor and detect surface displacement over large areas by utilizing the phase value of two observations separated in either time or space with millimetre accuracy (Colesanti *et al.*, 2003; Perissin and Rocca, 2006; Goel and Adam, 2014). Based on the previous studies, InSAR technique has been

used successfully to detect the movement or displacement caused by seismic events such as earthquakes (Massonnet and Feigl, 1993; Peltzer and Rosen, 1995) and volcanic eruptions ((Massonnet *et al.*, 1995; Remy *et. al.*, 2003). Common phenomena like landslides (Colesanti and Wasowski, 2006; Cascini *et al.*, 2010; Martire *et al.*, 2011; Herrera *et al.*, 2013), land subsidence (Jiang *et at*, 2010; Ferretti, 2000) and the characterization of behaviour of the surface motion in urban area (Webley *et al.*, 2002; Chen *et al.*, 2013; Colesanti *et al.*, 2003) have also been widely investigated over the time with this technique. As a matter of fact, this technique has been actively used to overcome the shortcomings of the ground-based measurement in remote area as well (Wang and Wright, 2012).

The technique of InSAR can be classified into two types *i.e*; i) along-track interferometry or known as single-pass interferometry, and ii) across-track interferometry or repeat-pass interferometry. It is well-known that the repeat-pass interferometry is the most sensitive to detect changes of the surface because the single-pass interferometry is taken under identical conditions at the same time; hence they are highly correlated, making it hard to determine the surface changes (Klees and Massonnet, 1999; Ebmeier *et., al.*, 2004). However, since the repeat-pass interferometry is acquired at different times, the images may be insufficient due to temporal and geometric decorrelation (Zebker and Villasenor,, 1992) and atmospheric artifacts (Zebker *et al.*, 1997; Hanssen, 1998; Hanssen, 2001).

The temporal decorrelation is caused by the temporal change in backscatter properties of the surface between the first and the second data acquisition, whereas geometrical decorrelation refers to the variations of reflectivity as a function of the incidence angle (Colesanti *et al.*, 2003; Perissin and Rocca, 2006). As for the atmospheric effects, the water vapour in the troposphere layer is actually introducing different delays at different times while signal is propagating through it (Noferini *et al.*, 2005). This atmospheric effect is not identical in different InSAR acquisitions, thus the effect cannot be easily cancelled out and leads additional shifts in phase signals (Li *et. al.*, 2005). Decorrelation often prevents InSAR from being an operational tool for surface deformation monitoring and topographic profile

reconstruction while interferogram images derived from repeat-pass spaceborne synthetic aperture radar systems exhibit artifacts due to the time and space variations of atmospheric water vapour which seriously affect the accuracy of the surface monitoring (Zebker *et al.*, 2007; Ferretti *et al.*, 2001).

The methods to mitigate the atmospheric delay in conventional InSAR data can be classified as 1) integration with dense GPS networks; 2) integration with multi-spectrum water vapor products, for example precipitable water vapor products from Moderate Resolution Imaging Spectroradiometer (MODIS) or Medium Resolution Imaging Spectrometer (MERIS); 3) integration with numerical weather forecast model, *e.g.* Weather Research and Forecast (WRF) model, and 4) using time-series InSAR techniques, *e.g.* Small Baseline Subset (SBAS), and Persistent Scatterer (PSInSAR) InSAR (Gong *et al.*, 2011). The GPS method often having difficulties in setting and maintaining GPS sites, while for optical satellite such as MODIS, a full water vapor column is hard to be obtained in most cases due to the persistent block from the clouds (Li *et al.*, 2005). Numerical weather model technique is usually required sufficient available boundary data in order to get accurate and better quality of the forecasts (Gong *et al.*, 2010). Furthermore, this method only aims to reconstruct the atmospheric state at SAR imagery acquisition time but do not solve the decorrelation problem in InSAR data.

However, studies found that time series InSAR technique is an attractive option that can address decorrelation as well as atmospheric artifacts since in most of the cases, it is impossible to remove or overcome these two problems by using an individual interferogram (Massonnet and Feigl, 1998; Sandwell and Price, 1998). The time series InSAR technique processes multiple acquisitions in time and exploits the statistic properties of atmospheric phase components in time series of SAR observations (Gong *et al.*, 2011). There are several time series approaches for InSAR application of deformation monitoring. However one of the commonly used approach of time series is known as Persistent Scatterer Interferometric Synthetic Aperture Radar (PSInSAR) technique which involves identifying “persistent scatterer” pixels whose scattering characteristics remain stable in time and when

viewed from different angles (Ferretti *et al.*, 2001; Hooper *et al.*, 2004; Hooper *et al.*, 2012; Kampes, 2005).

PSInSAR technique was first discovered in 1990s, where it utilizes the multi-interferogram framework of differential interferograms with respect to a single master image and estimates the displacement based on one or two dominant scatterers in the resolution cell (Ferretti *et al.*, 2000; Ferretti *et al.*, 2001). PSInSAR also takes benefits from isolated stable pixels which are almost unaffected by decorrelations within the resolution cell to estimate the atmospheric effects and mitigates it (Daniele and Fabio, 2006). The advantages of the PSInSAR technique can be seen from the several perspectives as compared to conventional InSAR (Ferretti *et al.*, 2001; Ferretti and Crespia, 2006; Velez *et al.*, 2011). But the drawback of this method is that it requires a large number of SAR acquisitions and prior knowledge of the study area properties (Tamburini *et al.*, 2010) although data requirement is not essentially a problem nowadays since there are many SAR sensors available, and data from these sensors can be obtained easily (Zibret *et al.*, 2012).

Nevertheless, there are various applications that exploit PSInSAR method such as land subsidence (Ferretti *et al.*, 2000), monitoring ground deformation (Colesanti *et al.*, 2003), developing high accuracy Digital Elevation Model (DEM) (Daniele and Fabio 2006) and detecting slow-landslide (Ferretti *et al.*, 2001). Several examples can be found in the literature where PSInSAR technique has been used for the monitoring of land subsidence in urban area. For example, Zhao *et al.*, (2009) had successfully identified an active zone for ground deformation in the urban area of Guangzhou city in South China using PSInSAR technique with the maximum subsidence or the rise rate showed from -26 to 20 milimeter/year. Meanwhile, a case study in Rotterdam, Netherlands, successfully identified urban subsidence due to gas extraction with a high PS density (159 PS/km<sup>2</sup>) where the displacement rates were detected up to 7 mm/year (Katelaar and Hanssen, 2003). PSInSAR also has a potential of monitoring the deformation of different types of infrastructure with high accuracy as demonstrated by Lan *et al.*, (2012) who classified PS points based on

their corresponding urban structure types successfully and shown the potential of using PInSAR technique to monitor the regular fluctuation of deformation rate of complex urban infrastructures in one fast developing area.

The discussion about the background study of this proposed topic can be concluded by restating that the land surface deformation monitoring is vital for various purpose especially monitoring the sustainability of urban infrastructures and this can be done using InSAR technique considering its long term data availability, large scale coverage, cloud penetration capability, low cost and most importantly the effectiveness in detecting surface movement deformation with high accuracy. However, this technique is bounded with two major limitations known as decorrelations and atmospheric disturbance that often limits the applicability of InSAR tool in monitoring accurate deformation. Nevertheless, these limitations can be successfully mitigated with the use of time series technique, PSInSAR that utilizes the stable pixels within the interferogram with high spatial density and produce better estimation accuracy. The PSInSAR technique is performed well in urban as well as non-urban areas; however, there are still scopes for improvement of measurement as the capability of this technique varies according to different circumstances.

## **1.2 Problem Statement**

The problem of ground deformation is quite obvious globally due to transformation of land cover, overexploitation of underground reservoir, natural disaster as well as massive infrastructure development. It is inevitable that any form of deformation can create potential risk for human life and properties, and this risk could be compounded if any damage of infrastructure occurs in urban areas due to the ground deformation. Therefore, it is essential to monitor the deformation or subsidence using an effective technology for the assessment of risk of urban subsidence, volcano dynamics, co-seismic and post seismic displacements along

faults, as well as slope instability especially when urban areas and infrastructures are involved (Ferronato *et. al*, 2006).

In Malaysia, there are a number of places such as Kuala Lumpur, Petaling Jaya, Ampang and Batu Caves which are growing very rapidly with the economic development and population growth. There are several reports that already indicated the problems in designing and maintaining the infrastructures of these cities. For example, the Petronas Twin Towers in Kuala Lumpur were shifted about 50 mm from their original planned positions due to intense fractures and limestone cavities in the foundation area (Ismail *et. al*, 2011). Furthermore, although Malaysia is generally safe from few natural disasters such as earthquake, typhoons and volcanic eruptions, nevertheless the country is still subjected to monsoon floods, sinkhole, landslides and land subsidence. The most common events in Malaysia are landslides which are triggered by rainfall or human activities on instable slopes and land subsidence due to over-pumping of ground water as happened in Ampang, Kuala Langat and Shah Alam areas (Stek, 2008). Although some big infrastructures in these cities may have been constructed with proper engineering and ground work, obviously many of the infrastructures have been build up without considering the risk of land deformation and need to be monitored in order to understand the probable risk and to take necessary precaution to avoid unexpected loss of property and life.

It is clear from the above circumstances that a continuous and long-term deformation monitoring system is required to identify hazardous areas and quantify the structural changes with quantitative interpretation to avoid the losses of properties and uncompensated lives. The use of space-born Synthetic Aperture Radar (SAR) is one of the best choices to monitor deformation for such a large area considering its long-term data availability, large-scale coverage and cloud-penetrating capability with a rather low cost. SAR data can be used for deformation monitoring using SAR interferometry (InSAR) technique. However, the only limiting factor of this technique is that the signal phase is sometimes biased with the

decorrelation problem and atmospheric contribution that introduce different delays at different times and in different points of the illuminated area (Noferini *et al.*, 2005).

Although there are many methods that can be applied to address these issues such as using GPS (Li *et al.*, 2005; Webley *et al.*, 2002), MODIS water vapour measurement (Foster *et al.*, 2006; Li *et al.*, 2005) and WRF model (Gong *et al.*, 2010); however, the advance technique of InSAR known as PSInSAR technique is the most attractive technique as it assists not only to overcome the decorrelation problems and atmospheric disturbance but it also has a capability in monitoring precise deformations that can hardly be achieved by using conventional technique by identifying the stable pixels based primarily on their phase variation in time (Lan *et al.*, 2012; Ferretti *et al.*, 2001; Kampes, 2005; Hooper *et al.*, 2006). The other particular interest of using PSInSAR technique is discriminating small scale features in such that various types of infrastructures are found in urban areas can be distinguished based on their spatial scale and enables the investigations of individual structural deformation (Crosetto *et al.*, 2010). Although the PSInSAR method is very effective in urban areas due to its main principle of selecting stable points which comes from permanent structures, there are still successful implementations of this technique for landslide monitoring (Sun *et al.*, 2015; Tantiaparp *et al.*, 2013), land subsidence (Li *et al.*, 2012) and slope assessment (Riddick *et al.*, 2012).

There are many PSInSAR algorithms available; however, the first PSInSAR algorithm has been developed in 2000 by Ferretti *et al.*, (2000), which further enhanced by Colesanti *et al.*(2003) and followed by Adam *et al.*, (2003); Crosetto *et al.*, (2003); Lyons and Sandwell, 2003; Werner *et al.*, (2002). In these algorithms, an initial set of PS pixels with a high signal-to-noise ratio (SNR) is identified by amplitude variation analysis and accept only the stable pixel which has similar phase history to the assumed model of deformation (Liu *et al.*, 2010). Nevertheless, Hooper *et al.*, (2007) stated that these approaches can fail due to two reasons *i.e.* i) the large distance between neighboring PS pixels, and ii) due to the deformation deviations from the model that are large which will make unwrapping become unreliable. Furthermore, these algorithms only consider the analysis of phase amplitude during

PS selection for which makes the identification of PS pixels generally becomes too low to obtain any reliable results in natural terrains which are generally have low SNR scatters (Meisina *et al.*, 2008).

In contrast, the Stanford Method for Permanent Scatterers (StaMPS), one kind of PSInSAR algorithm has extended the scope of PSInSAR to work effectively in urban as well as vegetated regions by incorporating spatial correlation of interferogram phase to find a network of stable pixels even with low amplitude stability without prior knowledge of temporal variations in the deformation (Marwa and Elisabeth, 2004; Hooper *et al.*, 2004; Hooper *et al.*, 2008; Liu *et al.*, 2010). In this algorithm, an initial filtering for the selection of PS pixels is done based on amplitude dispersion, and later the selection of PS pixel is finalized by several iterations of phase stability estimation and characterized the temporal model of deformation, rather than using an assumed model, which eliminates the need of a priori temporal model (Hooper *et al.*, 2007; Tiwari *et al.*, 2014). This approach is successful in finding PS pixels in both urban and non-urban areas, which makes it applicable in areas covered by forests and vegetation as well (Sousa, 2010).

Obviously, an effective PSInSAR algorithm requires several steps of processing for better estimation accuracy includes i) interferogram formation (data selection, image pairs, co-registration, phase unwrapping, *etc.*), ii) phase stability estimation, iii) phase selection, and iv) displacement estimation (Baer *et. al*, 1999; Hooper *et. al*, 2004; Hooper *et. al*, 2008). Although several studies have been made to retrieve reliable deformation parameters such as Vilaro *et al.*, (2010), Erten *et.al*, 2009 and Riddick *et al.*, (2012); nevertheless, these studies have only concentrated on the improvements of PSInSAR processing and mostly ignored the importance of other processing such as selection of data baselines, oversampling, co-registration, differential interferogram generation and geocoding. Furthermore, most of the studies are focused only on one type of terrain or land-use; hence the impact of the PSInSAR algorithm for different terrains is still remaining uncertain. In addition, no study has been conducted so far in Malaysia to monitor surface deformation in urban areas using InSAR technique.

Therefore, there is still a plenty of scope to evaluate or use this PSInSAR technique for monitoring the surface deformation or land subsidence in different land surface terrains (such as urban, vegetation, rural, mountain) considering not only PSInSAR processing technique but also effective procedure for the generation of enhance interferogram as well. However, this study investigates the surface deformation in Kuala Lumpur and nearby areas using PSInSAR technique considering the three important aspects *i.e.* i) the needs for the monitoring of deformation or land subsidence in this study area; ii) the effectiveness of InSAR technology for the monitoring deformation or land subsidence, and iii) finally the scope of the use of PSInSAR technology for the improvement of estimation accuracy by overcoming decorrelation and atmospheric effect. Necessity steps are going to be taken for the optimization of PS pixel selection in order to estimate deformation with high accuracy.

### **1.3 Research Objectives**

The main objective of this study is to monitor surface deformation in Kuala Lumpur and neighbouring areas using PSInSAR technique. The sub-objectives of this research are listed as below:

1. to demonstrate the effectiveness of PSInSAR technique for monitoring long-term deformation using L-band SAR
2. to explore the potential of optimization of PSInSAR processing parameters in order to get better estimation of surface deformation

These considerations lead to the formulation of three research questions related to the objectives stated above.

1. How effective is the PSInSAR technique in monitoring deformation?
2. Does the optimization process of PS pixel selection improve the estimation of deformation in the study area?

#### **1.4 Study Area**

In this study, Kuala Lumpur and neighbouring areas was selected to test and evaluate the performance of PSInSAR technique for monitoring surface deformation as can be seen in Figure 1.1.

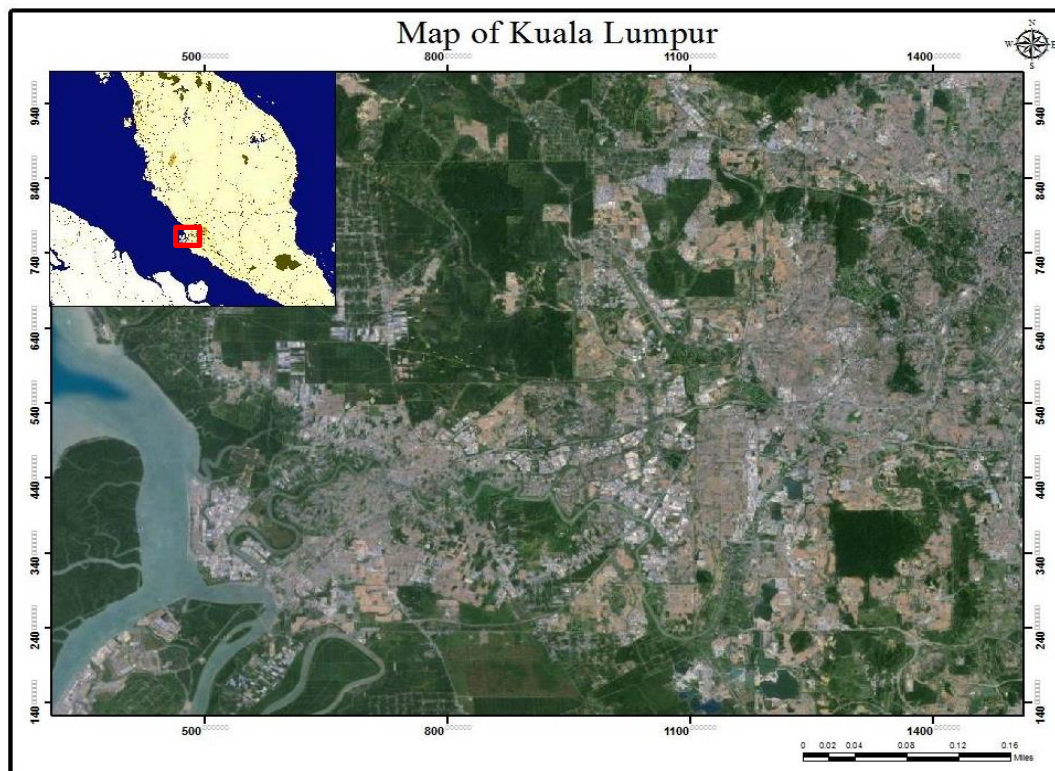


**Figure 1.1:** Location of Kuala Lumpur, Selangor

Kuala Lumpur (Figure 1.1), capital city of Malaysia, is considered as one of the fastest growing cities not only in Malaysia but also in South-East Asia. The land use in the study area is mainly peat swamp forest, plantation forest, inland forest, scrub, grassland, and ex-mining area (Konishi *et al.*, 2006). The landform of the area ranges from very flat terrain, especially for the peat swamp forest, ex-mining, grassland and scrub area, to quite hilly area for the natural forest ranging between 0 and 420 m above sea level (Lee and Pradhan, 2007). Majority of the land use pattern consist of built-up areas include commercial, residential, institution, industrial recreational area, infrastructure and utilities (Khaki *et al.*, 2014). Since Kuala Lumpur is the ex-mining area, the geologic settings of Kuala Lumpur is mainly composed of limestone bedrock with estimated 1,850m thick, overlying graphitic schist known as Hawthornden Schis, granitic hills, and mine waste deposits especially in the Bandar Sunway area, a suburban of Kuala Lumpur (Kong and Komoo, 1990). Many building sites on limestone areas in Kuala Lumpur have encountered a weak soil zone that could possibly leads to dangerous situation such as sudden collapse especially when this city is made of numerous new and tall

buildings, with modern and postmodern architecture that filled the skyline, such as the Petronas Twin Towers.

## 1.5 Scope of Study

1. This study used ALOS PALSAR from ascending satellite tracks covering from February 2007 to January 2011. This sensor operated in longer wavelength (L-band, 23.6 cm) with 46 days repeat cycle. In general, ALOS PALSAR has high spatial resolution (8m of FBS and 16 m of FBD) as compared to other sensors such as ERS1/2 (25 m) and Envisat ASAR (30 m). Moreover, L-band sensor operated in longer wavelength (23.6 cm); hence, a better penetration in an object, resulting in high quality interferograms.
2. Apart from radar data, this study used precise orbital data (PRC) for accurate co-registration process and generation of flatten interferogram. Besides that, an external Digital Elevation Model (DEM) also was used for the generation of differential interferogram. This study used DEM from Shuttle Radar Topography Mission (SRTM) (90m at ground worldwide).
3. In order to fully evaluate the capability of PSInSAR processing for monitoring the surface deformation (uplift or subsidence), several parts of the study area were considered with their terrain characteristics and detected PS densities.
4. For the improvement of overall accuracy of the results, an optimization process was followed during the generation of interferograms. This includes selection of images pairs (reducing perpendicular and temporal baseline as

well as Doppler centroid difference), accurate co-registration process and phase unwrapping process.

5. An optimization of PSInSAR processing parameters settings was also carried out to remove the noisy PS and to get stable PS points. The strategy helps to increase the density of detected persistent scatterers and reduce noise especially in deforming areas. Based on previous studies, the optimization was done considering several parameters *i.e.* 1) maximum acceptable spatial density (scatterers/km<sup>2</sup>) of selected pixels with random phase, 2) maximum standard deviation of the phase noise, 3) spatially correlated filtering time window, 4) unwrapping grid cell size, 5) coarser resample size and 6) maximum standard deviation of the resampled pixels of phase noise.
6. This study was carried out in several districts in Selangor located in Peninsular Malaysia which is composed by limestone formation, granitic hills, and mine waste deposits. The study area has been selected due to the need of monitoring deformation in these areas considering their geological settings that generally has weak foundation for construction work and developments.

## **1.6 Significance of Study**

The main contribution of this study is to evaluate the effectiveness of PSInSAR technique for monitoring deformation in different terrains, as current processes of conventional field based methods are too expensive, time consuming and requires long observation session considering the large area extend of the cities in order to get millimeter level accuracy (Genrich and Bock, 1992). Additionally, a long term land deformation monitoring using robust InSAR processing particularly

in the urban and sub-urban areas in Malaysia is hardly can be found in literature due to complexity of the processing technique and insufficient institutional support. Thus, findings from this study will promote the capabilities of PSInSAR technique as an important tool for surface deformation monitoring to quantify the structural changes in Malaysia together with quantitative interpretation. This technique (PSInSAR) can be optimized and eventually can be used potentially to assess hazards susceptibility at the regional scale with less effort as compared to other methods such as GPS.

In particular, this study is important as it can provide a fast and effective tool to local authorities to monitor ground deformation (slow/fast) and building behavior deformation at a relatively low cost. Slow deformation is usually hard to be detected as compared to fast deformation as it requires a long time observation. Hence, by taking the advantages of large achieves of radar data along with application of time-series technique such as PSInSAR, slow ground deformations as well as the historical deformation in the study areas can be easily detected and analyzed. This technique is particularly useful in Malaysia as the country is mostly suffered from slow deformations such as slow-landslides, subsidence, sinkhole and sediments which requires an accurate deformation analysis for implementing preventive measures. Furthermore, the use of PSInSAR for land deformation monitoring technique may also benefit the pace of development and maintenance of infrastructures in Malaysia by identifying safe areas for future infrastructures development which will ensure the safety of the civilians and the sustainability of the infrastructures.

## **1.7 Outline of Thesis**

The thesis consists of six (6) main chapters. The chapters are as follows:

## Chapter 1

This chapter which is the first chapter is basically a general overview of the research. This chapter introduces the report outlining the background of study, problem statement, study area, research objectives and significance of the research. The summaries of each chapter are also included in this chapter.

## Chapter 2

The second chapter is about literature reviews. This chapter describes the essential definition as well as the history of radar satellites, followed by basic principles of synthetic aperture radar and reviews of InSAR basic theory and PSInSAR principles. This chapter also includes the details regarding the atmospheric delay and decorrelation of the signal and the proven capabilities of PSInSAR techniques to successfully resolve the limitation of previous used technique and also attempt to reduce the atmospheric and decorrelation noise signal.

## Chapter 3

Third chapter discusses on the methodology and its procedures to fulfil the objectives of the research together with an overview methodology for validation of results. The DInSAR and PSInSAR processing are explained in details regarding the selected parameters and algorithm used in the processing based on the literature review, and the mathematical framework behind both processing are also included in Chapter 3.

## Chapter 4

Chapter 4 is on the analysis of PSInSAR results in the study area. The preliminary results given by default settings are discussed followed by the optimization of several parameters. The study area has been classified into ten different areas and detail analysis of final PSInSAR results on each area was briefly discussed.

### Chapter 5

Chapter 5 concentrated on the summarized and detailed discussion of the results using PSInSAR technique.

### Chapter 6

This chapter conclude the findings of the study. For future work and references, some recommendations and comments were noted down.

## REFERENCES

- Abdelfattah, R., & Nicolas, J. M. (2005). InSAR image co-registration using the Fourier–Mellin transform. *International Journal of Remote Sensing*, 26(13), 2865-2876.
- Abdikan, S., Hooper, A., Arikan, M., Balik Sanli, F., Cakir, Z., & Kemaldere, H. (2011). InSAR time series analysis of coal mining in Zonguldak city, Northwestern Turkey. In *Fringe Workshop*.
- Abdikan, S., Arikan, M., Sanli, F. B., & Cakir, Z. (2014). Monitoring of coal mining subsidence in peri-urban area of Zonguldak city (NW Turkey) with persistent scatterer interferometry using ALOS-PALSAR. *Environmental Earth Sciences*, 71(9), 4081-4089.
- Abidin, H. Z., Andreas, H., Kato, T., Ito, T., Meilano, I., Kimata, F & Harjono, H. (2009). Crustal deformation studies in Java (Indonesia) using GPS. *Journal of Earthquake and Tsunami*, 3(02), 77-88
- Abidin, H.Z. (1994). On-the-fly ambiguity resolution. *GPS World*, 5(4), 40-50.
- Briole, P., D. Massonnet, and C. Delacourt (1997), Post-eruptive deformation associated with the 1986-87 and 1989 lava flows of Etna detected by radar interferometry, *Geophysical Research Letters*, 24(1), 37-40.
- Adam, N., Kampes, B., Eineder, M., Worawattanamateekul, J., & Kircher, M. (2003). The development of a scientific permanent scatterer system. In *ISPRS Workshop High Resolution Mapping from Space, Hannover, Germany*(Vol. 2003, p. 6).

- Agram, P., Jolivet, R., Simons, M., and Riel, B. (2012). GIAN-T-Generic InSAR Analysis Toolbox. In *AGU Fall Meeting Abstracts* (Vol. 1, p. 0897).
- Akcin, H., Kutoglu, H. S., Kemaldere, H., Deguchi, T., & Koksall, E. (2010). Monitoring subsidence effects in the urban area of Zonguldak Hardcoal Basin of Turkey by InSAR-GIS integration. *Natural Hazards and Earth System Sciences*, 10(9), 1807-1814.
- Al-Ani, H., Oh, E., & Chai, G. (2013). Characteristics of embedded peat in coastal environments. *International Journal of Geo-mate*, 5(1), 609618.
- Alazzi, B., Alparone, L., & Baronti, S. (1999). Reliably estimating the speckle noise from SAR data. In *Geoscience and Remote Sensing Symposium, 1999. IGARSS'99 Proceedings. IEEE 1999 International* (Vol. 3, pp. 1546-1548). IEEE.
- Althuwaynee, O. F., Pradhan, B., & Lee, S. (2012). Application of an evidential belief function model in landslide susceptibility mapping. *Computers & Geosciences*, 44, 120-135.
- Amelung, F., & Day, S. (2002). InSAR observations of the 1995 Fogo, Cape Verde, eruption: Implications for the effects of collapse events upon island volcanoes. *Geophysical research letters*, 29(12), 47-1.
- Aobpaet, A., Cuenca, M. C., & Trisirisatayawong, I. (2009, October). PS-InSAR Measurement of Land Subsidence in Bangkok Metropolitan Area. In *the 30th Asian Conference on Remote Sensing* (pp. 18-23)
- Ashraf, M. A., Maah, M. J., & Yusoff, I. (2011). Heavy metals accumulation in plants growing in ex tin mining catchment. *International Journal of Environmental Science & Technology*, 8(2), 401-416.
- Ashraf, H., & Cawood, F. (2015). Geospatial subsidence hazard modelling at Sterkfontein Caves. *South African Journal of Geomatics*, 4(3), 273-284.
- Atzori, S., Hunstad, I., Chini, M., Salvi, S., Tolomei, C., Bignami, C., ... & Boschi, E. (2009). Finite fault inversion of DInSAR coseismic displacement of the 2009 L'Aquila earthquake (central Italy). *Geophysical Research Letters*, 36(15)
- Ashkenazi, V., Dodson, A.H., Sykes, R.M., Crane, S.A. (1980) Remote measurement of ground movements by surveying techniques *Civil Eng. Survey.*, 5 (4), pp. 15–22

- Aung Lwin; *Geomorphological Mapping With Respect To Amplitude, Coherence and Phase Information Of ERS SAR Tandem Pair*, 2008, The International Archives of the Photogrammetry, Remote Sensing and Spatial Information Sciences. Vol. XXXVII. Part B8. Beijing, Commission VIII, WG VIII/12
- Baby, H., Gole, P., and Lavergnat, J., A., Model for tropospheric excess path length of radio waves from surface meteorological measurements, *Radio Sci.*, 22, 1023-1038, 1988.
- Baer, G., Sandwell, D., Williams, S., Bock, Y., & Shamir, G. (1999). Coseismic deformation associated with the November 1995,  $M_w = 7.1$  Nuweiba earthquake, Gulf of Elat (Aqaba), detected by synthetic aperture radar interferometry. *Journal of Geophysical Research*, 104(25), 221425.
- Balaji, P. M. (2011). Estimation and Correction of Tropospheric and Ionospheric Effects on Differential SAR Interferograms. *M. Sc., Indian Institute of Remote Sensing (IIRS) and International Institute for Geoinformation Science and Earth Observation (ITC)*.
- Bamler, Richard, and Philipp Hartl. "Synthetic aperture radar interferometry." *Inverse problems* 14.4 (1998): R1.
- Bara, M., Broquetas, A., Scheiber, R., & Horn, R. (2000, December). Geocoding techniques for interferometric and polarimetric airborne SAR data. In *Europto Remote Sensing* (pp. 279-290). International Society for Optics and Photonics.
- Baselice, F., Budillon, A., Ferraioli, G., & Pascazio, V. (2009). Layover solution in SAR imaging: A statistical approach. *Geoscience and Remote Sensing Letters, IEEE*, 6(3), 577-581
- Beauducel, F., Briole, P., & Froger, J. L. (2000). Volcano-wide fringes in ERS synthetic aperture radar interferograms of Etna (1992–1998): Deformation or tropospheric effect?. *Journal of Geophysical Research: Solid Earth (1978–2012)*, 105(B7), 16391-16402.

- Bennett, Andrew J., and David Blacknell. "The extraction of building dimensions from high resolution SAR imagery." Radar Conference, 2003. Proceedings of the International. IEEE, 2003.
- Berardino, P., Fornaro, G., Lanari, R., & Sansosti, E. (2002). A new algorithm for surface deformation monitoring based on small baseline differential SAR interferograms. *Geoscience and Remote Sensing, IEEE Transactions on*, 40(11), 2375-2383.
- Bevis, M., Businger, S., Chiswell, S., Herring, T. A., Anthes, R. A., Rocken, C., & Ware, R. H. (1994). GPS meteorology: Mapping zenith wet delays onto precipitable water. *Journal of applied meteorology*, 33(3), 379-386.
- Biggs, J., Bergman, E., Emmerson, B., Funning, G. J., Jackson, J., Parsons, B., and Wright, T. J. (2006). Fault identification for buried strike-slip earthquakes using InSAR: The 1994 and 2004 Al Hoceima, Morocco earthquakes. *Geophysical Journal International*, 166(3), 1347-1362.
- Bondár, I., and K. McLaughlin (2009), Seismic location bias and uncertainty in the presence of correlated and non-Gaussian travel-time errors, *Bull. Seismol. Soc. Am.*, 99, 172–193.
- Bonforte, A., Ferretti, A., Prati, C., Puglisi, G., & Rocca, F. (2001). Calibration of atmospheric effects on SAR interferograms by GPS and local atmosphere models: first results. *Journal of Atmospheric and Solar-Terrestrial Physics*, 63(12), 1343-1357.
- Bonnard, Ch., Noverraz, F., Dupraz, H. (1996), Long-term movements of substabilized versants and climatic changes in the Swiss Alps ,in: K. Senneset (Ed.), Proc. 7th Int. Symp. on Landslides, Trondheim, Vol. 3, pp. 1525–1530
- Bryksin, V. M., Filatov, A. V., Yevtyushkin, A. V., Брыксин, В. М., Филатов, А. В., & Евтюшкин, А. В. (2012). Using of SAR data and DInSar-PSInSar technique for monitoring Western Siberia and Arctic. *Журнал радиоэлектроники*, (6), 1-53.
- Buckheit, J. B., and D. L. Donoho (1995), WaveLab and reproducible research, report, 27 pp., Dep. of Stat., Stanford Univ., Stanford, Calif

- Bürgmann, Roland, et al. "Earthquake potential along the northern Hayward fault, California." *Science* 289.5482 (2000): 1178-1182.
- Brain, M., & Harris, T. (2011). How GPS receivers work.
- Briole, P., D. Massonnet, and C. Delacourt (1997), Post-eruptive deformation associated with the 1986-87 and 1989 lava flows of Etna detected by radar interferometry, *Geophysical Research Letters*, 24(1), 37-40.
- Carballo, G. F., & Fieguth, P. W. (2000). Probabilistic cost functions for network flow phase unwrapping. *Geoscience and Remote Sensing, IEEE Transactions on*, 38(5), 2192-2201.
- Capková, I., Kianicka, J., & Halounová, L. (2005). New results of interferometric processing of the northern Bohemia scenes.
- Cascini, L., Fornaro, G., & Peduto, D. (2010). Advanced low-and full-resolution DInSAR map generation for slow-moving landslide analysis at different scales. *Engineering Geology*, 112(1), 29-42.
- Catalão, J., Nico, G., Hanssen, R., & Catita, C. (2011). Merging GPS and atmospherically corrected InSAR data to map 3D terrain displacement velocity. *IEEE transactions on geoscience and remote sensing*, 49(6), 2354-2360.
- Cattabeni, M., Monti-Guarnieri, A., & Rocca, F. (1994, August). Estimation and improvement of coherence in SAR interferograms. In *INTERNATIONAL GEOSCIENCE AND REMOTE SENSING SYMPOSIUM* (Vol. 2, pp. 720-720). INSTITUTE OF ELECTRICAL & ELECTRONICSENGINEERS, INC (IEE).
- Chapin, E., Chan, S. F., Chapman, B. D., Chen, C. W., Martin, J. M., Michel, T. R., ... & Rosen, P. A. (2006, April). Impact of the ionosphere on an L-band space based radar. In *Radar, 2006 IEEE Conference on* (pp. 8-pp). IEEE.
- Chaussard, E., Amelung, F., Abidin, H., & Hong, S. H. (2013). Sinking cities in Indonesia: ALOS PALSAR detects rapid subsidence due to groundwater and gas extraction. *Remote Sensing of Environment*, 128, 150-161.

- Chen, A. C. (2013). *L-Band INSAR estimates of Greenland ice sheet accumulation rates* (Doctoral dissertation, Stanford University). Colesanti, C., Ferretti, A., Prati, C., & Rocca, F. (2003). Monitoring landslides and tectonic motions with the Permanent Scatterers Technique. *Engineering Geology*, 68(1), 3-14.
- Chen, J., & Zebker, H. A. (2012). Ionospheric artifacts in simultaneous L-band InSAR and GPS observations. *Geoscience and Remote Sensing, IEEE Transactions on*, 50(4), 1227-1239.
- Chen, H. M., Arora, M. K., & Varshney, P. K. (2003). Mutual information-based image registration for remote sensing data. *International Journal of Remote Sensing*, 24(18), 3701-3706.
- Colesanti, C., and Wasowski, J. (2006). Investigating landslides with space-borne Synthetic Aperture Radar (SAR) interferometry. *Engineering geology*, 88(3), 173-199.
- Colesanti, C., Ferretti, A., Prati, C., & Rocca, F. (2003). Monitoring landslides and tectonic motions with the Permanent Scatterers Technique. *Engineering Geology*, 68(1), 3-14.
- Collini, M., Hu, B., Jetter, J., Miller, C. P., Unwalla, R. J., Keith Jr, J. C., ... & Basso, M. (2006, March). Discovery and SAR of phenyl-acetic acid based substituted quinolines as liver X receptor (LXR) agonists. In *ABSTRACTS OF PAPERS OF THE AMERICAN CHEMICAL SOCIETY* (Vol. 231). 1155 16TH ST, NW, WASHINGTON, DC 20036 USA: AMER CHEMICAL SOC.
- Crosetto, M., Tarantola, S., & Saltelli, A. (2000). Sensitivity and uncertainty analysis in spatial modelling based on GIS. *Agriculture, ecosystems & environment*, 81(1), 71-79.
- Crosetto, M. (2002). Calibration and validation of SAR interferometry for DEM generation. *ISPRS Journal of Photogrammetry and Remote Sensing*, 57(3), 213-227.
- Crosetto M, Crippa B, Biescas E, Monserrat O, Agudo M, Fernández P. (2005) Land deformation monitoring using SAR interferometry: state-of-the-art. *Photogramm. Fernerkundung Geoinformation* 6:497-510.

- Crosetto, M., A. Arnaud, J. Duro, E. Biescas, and M. Agudo (2003), Deformation monitoring using remotely sensed radar interferometric data, paper presented at 11th FIG Symposium on Deformation Measurements, Patras Univ., Santorini,
- Crosetto, M., Monserrat, O., Iglesias, R., & Crippa, B. (2010). Persistent scatterer interferometry. *Photogrammetric Engineering & Remote Sensing*, 76(9), 1061-1069.
- Crosta, G. B., Allievi, J., Frattini, P., Giannico, C., & Lari, S. (2008). Monitoring deep-seated gravitational slope deformations in the Alps by PSInSAR techniques. In *Geophysical Research Abstracts* (Vol. 10).
- Curlander, J. C., & McDonough, R. N. (1991). Synthetic aperture radar (p. 396). John Wiley & Sons
- David, K. (1995). Design of routing networks using geographic information systems: Applications to solid and hazardous waste transportation planning.
- De Clercq, P. Y., Devleeschouwer, X., & Pouriel, F. (2006, February). Subsidence revealed by PSInSAR technique in the Ottignies-Wavre area (Belgium) related to water pumping in urban area. In *Fringe 2005 Workshop*(Vol. 610).
- Dehghani, M., Zojj, M. J. V., Hooper, A., Hanssen, R. F., Entezam, I., & Saatchi, S. (2013). Hybrid conventional and Persistent Scatterer SAR interferometry for land subsidence monitoring in the Tehran Basin, Iran. *ISPRS journal of photogrammetry and remote sensing*, 79, 157-170.
- Delacourt, C., Briole, P., & Achache, J. A. (1998). Tropospheric corrections of SAR interferograms with strong topography. Application to Etna. *Geophysical Research Letters*, 25(15), 2849-2852.
- Dewaele, P., Wambacq, P., Oosterlinck, A., & Marchand, J. L. (1990, May). Comparison of some speckle reduction techniques for SAR images. In *Geoscience and Remote Sensing Symposium, 1990. IGARSS'90. 'Remote Sensing Science for the Nineties', 10th Annual International* (pp. 2417-2422). IEEE.

- Dick, H. W., & Rimmer, P. J. (1998). Beyond the third world city: the new urban geography of South-east Asia. *Urban Studies*, 35(12), 2303-2321.
- Ding, X. L., Liu, G. X., Li, Z. W., Li, Z. L., & Chen, Y. Q. (2004). Ground subsidence monitoring in Hong Kong with satellite SAR interferometry. *Photogrammetric Engineering & Remote Sensing*, 70(10), 1151-1156.
- Doin, M. P., Lasserre, C., Peltzer, G., Cavalié, O., and Doubre, C. (2009). Corrections of stratified tropospheric delays in SAR interferometry: Validation with global atmospheric models. *Journal of Applied Geophysics*, 69(1), 35-50.
- Dong, D., T. A. Herring, and R. W. King (1998), Estimating regional deformation from a combination of space and terrestrial geodetic data, *J. Geodesy*, 72, 200–214.
- Dong, D., P. Fang, Y. Bock, M. K. Cheng, and S. Miyazaki (2002), Anatomy of apparent seasonal variations from GPS-derived site position time series, *J. Geophys. Res.*, 107(B4), 2075,
- Doris (2008), “Delft Object-oriented Radar Interferometric Software User’s manual and technical documentation”, *Delft Institute of Earth Observation and Space Systems (DEOS) Delft University of Technology*
- Ebmeier, S. K., Biggs, J., Mather, T. A., & Amelung, F. (2013). On the lack of InSAR observations of magmatic deformation at Central American volcanoes. *Journal of Geophysical Research: Solid Earth*, 118(5), 2571-2585.
- Eichel, P., & Ives, R. W. (1999). *Compression of complex-valued SAR images. Image Processing, IEEE Transactions on*, 8(10), 1483-1487.
- Emardson, T. R., Simons, M., & Webb, F. H. (2003). *Neutral atmospheric delay in interferometric synthetic aperture radar applications: Statistical description and mitigation. Journal of Geophysical Research: Solid Earth (1978–2012)*, 108(B5).

- Erten, E., Reigber, A., & Hellwich, O. (2010). Generation of three-dimensional deformation maps from InSAR data using spectral diversity techniques. *ISPRS Journal of Photogrammetry and Remote Sensing*, 65(4), 388-394.
- ESA, 2007; ASAR products user guide; ENVISAT ASAR Product Handbook (2007)
- EOS, Agram, P. S., Jolivet, R., Riel, B., Lin, Y. N., Simons, M., Hetland, E., and Lasserre, C. (2013). New radar interferometric time series analysis toolbox released. *Eos, Transactions American Geophysical Union*, 94(7), 69-70.
- Ferretti, A., Prati, C., Rocca, F., & Monti Guarnieri, A. (1997). Multibaseline SAR interferometry for automatic DEM reconstruction (DEM). In Third ERS Symposium on Space at the service of our Environment (Vol. 414, p. 1809)
- Ferretti, A., Prati, C., & Rocca, F. (2000). Nonlinear subsidence rate estimation using permanent scatterers in differential SAR interferometry. *Geoscience and Remote Sensing, IEEE transactions on*, 38(5), 2202-2212.
- Ferretti, A., Prati, C., & Rocca, F. (2001). Permanent scatterers in SAR interferometry. *Geoscience and Remote Sensing, IEEE Transactions on*, 39(1), 8-20.
- Ferretti, A., & Crippa, S. (2006, October). Advances in differential SAR interferometry: from DInSAR to PSInSAR. In *Proceedings of the CSTARTS "height" workshop*.
- Ferronato, M., Gambolati, G., Teatini, P., & Baù, D. (2006). Stochastic poromechanical modeling of anthropogenic land subsidence. *International journal of solids and structures*, 43(11), 3324-3336.
- Fornaro, G., Pauciuolo, A., & Serafino, F. (2009). Deformation monitoring over large areas with multipass differential SAR interferometry: a new approach based on the use of spatial differences. *International Journal of Remote Sensing*, 30(6), 1455-1478.
- Foster, J., Brooks, B., Cherubini, T., Shacat, C., Businger, S., & Werner, C. L. (2006). Mitigating atmospheric noise for InSAR using a high resolution weather model. *Geophysical Research Letters*, 33(16).

- Frey, O., Hajnsek, I., & Wegmuller, U. (2013, July). Spaceborne SAR tomography in urban areas. In 2013 *IEEE International Geoscience and Remote Sensing Symposium-IGARSS* (pp. 69-72). IEEE.
- Goldstein R., H. Engelhardt, B. Kamb and R. Frolich (1993). Satellite radar interferometry for monitoring ice sheet motion: Application to an Antarctic ice stream. *Science*, 262, 1525- 1530
- Gabriel, A. K., & Goldstein, R. M. (1988). Crossed orbit interferometry: theory and experimental results from SIR-B. *International Journal of Remote Sensing*,9(5), 857-872.
- Gatelli, F., Guamieri, A. M., Parizzi, F., Pasquali, P., Prati, C., & Rocca, F. (1994). The wavenumber shift in SAR interferometry. *Geoscience and Remote Sensing, IEEE Transactions on*, 32(4), 855-865
- Genrich, J. F., & Bock, Y. (1992). Rapid resolution of crustal motion at short ranges with the Global Positioning System. *Journal of Geophysical Research: Solid Earth (1978–2012)*, 97(B3), 3261-3269.
- Gens, R. (2003). Two-dimensional phase unwrapping for radar interferometry: developments and new challenges. *International Journal of Remote Sensing*,24(4), 703-710.
- Goel, K., & Adam, N. (2014). Fusion of monostatic/bistatic InSAR stacks for urban area analysis via distributed scatterers.
- Gong, W., Meyer, F., Webley, P. W., Morton, D., & Liu, S. (2010, July). Performance analysis of atmospheric correction in InSAR data based on the Weather Research and Forecasting Model (WRF). In *Geoscience and Remote Sensing Symposium (IGARSS), 2010 IEEE International* (pp. 2900-2903). IEEE.
- Gong, P., Li, Z., Huang, H., Sun, G., & Wang, L. (2011). ICESat GLAS data for urban environment monitoring. *Geoscience and Remote Sensing, IEEE Transactions on*, 49(3), 1158-1172.
- Gong, W., et al., 2015. Temporal filtering of InSAR data using statistical parameters from NWP models. *IEEE Transactions on Geoscience and Remote Sensing*, 53 (7), 4033–4044. doi:10.1109/TGRS.2015.2389143

- Gonzalez, Pablo J., and Jose Fernandez. "Error estimation in multitemporal InSAR deformation time series, with application to Lanzarote, Canary Islands." *Journal of Geophysical Research: Solid Earth* (1978–2012) 116.B10 (2011).
- Gulla, G., Nicoletti, G., M. Sorriso-Valvo (1988), A portable device for measuring displacements along fractures Proc. 5th Int. Symp. on Landslides, Lausanne, Vol. 1, pp. 423–426
- Gupta, P., R. Hasan, and U. Kumar. 2009. "Big Reforms but Small Payoffs: Explaining the Weak Record of Growth in Indian Manufacturing" in S. Bery, B. Bosworth, and A. Panagariya (eds), *India Policy Forum*, volume 5, pp 59-108.
- Gupta, M., & Srivastava, P. K. (2010). Integrating GIS and remote sensing for identification of groundwater potential zones in the hilly terrain of Pavagarh, Gujarat, India. *Water International*, 35(2), 233-245
- Hassaballa, A. A., Althuwaynee, O. F., & Pradhan, B. (2014). Extraction of soil moisture from RADARSAT-1 and its role in the formation of the 6 December 2008 landslide at Bukit Antarabangsa, Kuala Lumpur. *Arabian Journal of Geosciences*, 7(7), 2831-2840.
- Hanssen, R.F., P.J.G. Teunissen and P. Joosten (2001). Phase Ambiguity Resolution for Stacked Radar Interferometric Data, Proceedings of the International Symposium on Kinematic Systems in Geodesy, Geomatics and Navigation, Banff, Canada, 5-8 June, 317-320
- Hansen, P. C. (1994), A Matlab package for analysis and solution of discrete ill-posed problems, *Numer. Algorithms*, 6, 1–35.
- Hanssen, R. F. (2001). *Radar interferometry: data interpretation and error analysis* (Vol. 2). Springer Science & Business Media.
- Hanssen, R., & Bamler, R. (1999). Evaluation of interpolation kernels for SAR interferometry. *IEEE Transactions on Geoscience and Remote Sensing*, 37(1), 318-321.
- Hansen, P. C. (2007), Regularization tools version 4.0 for Matlab 7.3, *Numer. Algorithms*, 46, 184–194.

- Herrera, G., Gutiérrez, F., García-Davalillo, J. C., Guerrero, J., Notti, D., Galve, J. P., ... & Cooksley, G. (2013). Multi-sensor advanced DInSAR monitoring of very slow landslides: The Tena Valley case study (Central Spanish Pyrenees). *Remote Sensing of Environment*, 128, 31-43.
- Hetland, E. A., Musé, P., Simons, M., Lin, Y. N., Agram, P. S., & DiCaprio, C. J. (2012). Multiscale InSAR time series (MInTS) analysis of surface deformation. *Journal of Geophysical Research: Solid Earth (1978–2012)*, 117(B2).
- Hellwich, O., & Ebner, H. (2000). Geocoding SAR interferograms by least squares adjustment. *ISPRS Journal of Photogrammetry and Remote Sensing*, 55(4), 277-288.
- Hellwich, Olaf, Manfred Günzl, and Christian Wiedemann. "Fusion of optical imagery and SAR/INSAR data for object extraction." *International Archives of Photogrammetry and Remote Sensing* 33.B3/1; PART 3 (2000): 389-396.
- Herring, T. A., J. L. Davis, and I. I. Shapiro (1990), Geodesy by radio interferometry: The application of Kalman filtering to the analysis of very long baseline interferometry data, *J. Geophys. Res.*, 95, 12,561–12,581.
- Hesterberg, T., Moore, D. S., Monaghan, S., Clipson, A., & Epstein, R. (2005). Bootstrap methods and permutation tests. *Introduction to the Practice of Statistics*, 5, 1-70.
- Hetland, E. A., Musé, P., Simons, M., Lin, Y. N., Agram, P. S., and DiCaprio, C. J. (2012). Multiscale InSAR time series (MInTS) analysis of surface deformation. *Journal of Geophysical Research: Solid Earth (1978–2012)*, 117(B2).
- Hilley, G. E., Bürgmann, R., Ferretti, A., Novali, F., & Rocca, F. (2004). Dynamics of slow-moving landslides from permanent scatterer analysis. *Science*, 304(5679), 1952-1955.
- Hoffmann, J. (2003). *The application of satellite radar interferometry to the study of land subsidence over developed aquifer systems.*

- Holecz, Francesco, et al. "Height model generation, automatic geocoding and a mosaicing using airborne AeS-1 InSAR data." *Geoscience and Remote Sensing, 1997. IGARSS'97. Remote Sensing-A Scientific Vision for Sustainable Development., 1997 IEEE International*. Vol. 4. IEEE, 1997.
- Hooper, Andrew John. *Persistent scatter radar interferometry for crustal deformation studies and modeling of volcanic deformation*. 2006.
- Hooper, Andrew, and Howard A. Zebker. "Phase unwrapping in three dimensions with application to InSAR time series." *JOSA A* 24.9 (2007): 2737-2747.
- Hooper, A. (2008). A multi-temporal InSAR method incorporating both persistent scatterer and small baseline approaches. *Geophysical Research Letters*, 35(16).
- Hooper, A., Bekaert, D., Spaans, K., & Arikan, M. (2012). Recent advances in SAR interferometry time series analysis for measuring crustal deformation. *Tectonophysics*, 514, 1-13.
- Hooper, A., Segall, P., & Zebker, H. (2007). Persistent scatterer interferometric synthetic aperture radar for crustal deformation analysis, with application to Volcán Alcedo, Galápagos. *Journal of Geophysical Research: Solid Earth (1978–2012)*, 112(B7).
- Hooper, A., Zebker, H., Segall, P., & Kampes, B. (2004). A new method for measuring deformation on volcanoes and other natural terrains using InSAR persistent scatterers. *Geophysical research letters*, 31(23).
- Hsu, L., & Bürgmann, R. (2006). Surface creep along the Longitudinal Valley fault, Taiwan from InSAR measurements. *Geophysical research letters*, 33(6).
- Huang, Q. H., & He, X. F. (2005). Introduction of earth deformations by D-InSAR. *GNSS World of China*, 30(3), 19-23.
- Huby, M. (2001). The sustainable use of resources on a global scale. *Social Policy & Administration*, 35(5), 521-537.
- Humme, A. (2007), Point Density Optimization for SAR Interferometry; a Study Tested on Salt Mine Areas, Master's thesis, Delft University of Technology

- Ismail, S. , Mansor, S., Rodsi, A., & Bujang, B. K. (2011). Geotechnical modeling of fractures and cavities that are associated with geotechnical engineering problems in Kuala Lumpur limestone, Malaysia. *Environmental Earth Sciences*, 62(1), 61-68.
- Jensen, J. R., and Cowen, D. C. (1999). Remote sensing of urban/suburban infrastructure and socio-economic attributes. *Photogrammetric engineering and remote sensing*, 65, 611-622.
- Jezek, K. C., Liu, H., Zhao, Z., & Li, B. (1999). Improving a digital elevation model of Antarctica using radar remote sensing data and GIS techniques 1. *Polar Geography*, 23(3), 185-200..
- Jha, B., Bottazzi, F., Wojcik, R., Coccia, M., Bechor, N., McLaughlin, D., ... & Juanes, R. (2015). Reservoir characterization in an underground gas storage field using joint inversion of flow and geodetic data. *International Journal for Numerical and Analytical Methods in Geomechanics*, 39(14), 1619-1638.
- Jiang, L.M., Lin, H., Zhao, Q., (2010), Long-term reclamation settlement of Chek Lap Kok Airport, Hong Kong: Insights from advanced InSAR technique and geotechnical investigations *Engineering Geology*, 110, pp. 77–92
- Jiang, L., Lin, H., Ma, J., Kong, B., & Wang, Y. (2011). Potential of small-baseline SAR interferometry for monitoring land subsidence related to underground coal fires: Wuda (Northern China) case study. *Remote Sensing of Environment*, 115(2), 257-268.
- John d'Errico (2006). <http://www.mathworks.com/matlabcentral/fileexchange/4551>
- Johnsen, H., L. Lauknes, et al, 1995. Geocoding of Fast-delivery ERS-1 SAR Image Mode Product Using DEM Data. *International Journal of Remote Sensing*. 16(11), pp.1957-1968.
- Jolivet, R., Grandin, R., Lasserre, C., Doin, M. P., and Peltzer, G. (2011). Systematic InSAR tropospheric phase delay corrections from global meteorological reanalysis data. *Geophysical Research Letters*, 38(17).
- Joughin, I., Das, S. B., King, M. A., Smith, B. E., Howat, I. M., & Moon, T. (2008). Seasonal speedup along the western flank of the Greenland Ice Sheet. *Science*, 320(5877), 781-783.

- Jung, H. S., Lee, D. T., Lu, Z., & Won, J. S. (2013). Ionospheric correction of SAR interferograms by multiple-aperture interferometry. *Geoscience and Remote Sensing, IEEE Transactions on*, 51(5), 3191-3199.
- Kampes, B., & Usai, S. (1999, August). Doris: The delft object-oriented radar interferometric software. In *2nd international symposium on operationalization of remote sensing, enschede, the netherlands* (Vol. 16, p. 20).
- Kampes, B. M., Hanssen, R. F., & Perski, Z. (2003, December). Radar interferometry with public domain tools. In *Proceedings of FRINGE* (pp. 1-5)
- Kampes, 2005. B.M. Kampes. Radar Interferometry: Persistent Scatterer Technique, Springer, Germany (2005)
- Kampes, B. M. (2006). *Radar interferometry*. Springer.
- Ketelaar, V. B. H., & Hanssen, R. F. (2003, December). Separation of different deformation regimes using PS-INSAR data. In *Proceedings of FRINGE* (pp. 1-5).
- Khaki, M., Yusoff, I., & Islami, N. (2014). Groundwater quality assessment of a freshwater wetland in the Selangor (Malaysia) using electrical resistivity and chemical analysis. *Water Science and Technology: Water Supply*, 14(2), 255-264.
- Kim, S. W., Lee, C. W., Song, K. Y., Min, K. D., & Won, J. S. (2005). Application of L-band differential SAR interferometry to subsidence rate estimation in reclaimed coastal land. *International journal of remote sensing*, 26(7), 1363-1381.
- Kim, J. S., Kim, D. J., Kim, S. W., Won, J. S., & Moon, W. M. (2007). Monitoring of urban land surface subsidence using PSInSAR. *Geosciences Journal*, 11(1), 59-73.
- Kim, S. W., Wdowinski, S., Dixon, T. H., Amelung, F., Kim, J. W., & Won, J. S. (2010). Measurements and predictions of subsidence induced by soil consolidation using persistent scatterer InSAR and a hyperbolic model. *Geophysical Research Letters*, 37(5)

- Kim, J. H., Younis, M., Moreira, A., & Wiesbeck, W. (2013). A novel OFDM chirp waveform scheme for use of multiple transmitters in SAR. *IEEE Geoscience and Remote Sensing Letters*, 10(3), 568-572.
- Klees and Massonnet, 1999, R. Klees, D. Massonnet. (1999). Deformation measurements using SAR interferometry: potential and limitations. *Geol. Minjbouw*, 77 pp. 161–176
- Kohlhase, A. O., Feigl, K. L., & Massonnet, D. (2003). Applying differential InSAR to orbital dynamics: a new approach for estimating ERS trajectories. *Journal of Geodesy*, 77(9), 493-502.
- Konishi, S., Tani, M., Kosugi, Y., Takanashi, S., Sahat, M. M., Nik, A. R., ... & Okuda, T. (2006). Characteristics of spatial distribution of throughfall in a lowland tropical rainforest, Peninsular Malaysia. *Forest Ecology and Management*, 224(1), 19-25.
- Kong, T. B., & Komoo, I. (1990). Urban geology: case study of Kuala Lumpur, Malaysia. *Engineering geology*, 28(1-2), 71-94.
- Kotsis, I., Kontoes, C., Paradissis, D., Karamitsos, S., Elias, P., & Papoutsis, I. (2008). A methodology to validate the InSAR derived displacement field of the September 7th, 1999 Athens earthquake using terrestrial surveying. improvement of the assessed deformation field by interferometric stacking. *Sensors*, 8(7), 4119-4134.
- Krzanowski, W. J., P. Jonathan, W. V. McCarthy, and M. R. Thomas (1995), Analysis with singular covariance matrices: Methods and applications to spectroscopic data, *J. R. Stat. Soc., Ser. C*, 44, 101–115.
- Lan, H., Li, L., Liu, H., & Yang, Z. (2012). Complex urban infrastructure deformation monitoring using high resolution PSI. *IEEE Journal of Selected Topics in Applied Earth Observations and Remote Sensing*, 5(2), 643-651.
- Lanari, R., Lundgren, P., Manzo, M., & Casu, F. (2004). Satellite radar interferometry time series analysis of surface deformation for Los Angeles, California. *Geophysical Research Letters*, 31(23).

- Lauknes, T. R., Zebker, H. A., & Larsen, Y. (2011). InSAR deformation time series using an-norm small-baseline approach. *IEEE Transactions on Geoscience and Remote Sensing*, 49(1), 536-546.
- Lee S, Pradhan B (2006) Probabilistic landslide hazards and risk mapping on Penang Island, Malaysia. *J Earth Syst Sci* 115:661–672
- Lee S, Pradhan B (2007) Landslide hazard mapping at Selangor, Malaysia using frequency ratio and logistic regression models. *Landslides* 4:33–41
- Lee, Y. J., & Yoo, C. S. (2007). Subsurface settlement profiles above shallow and deep model tunnels at large ground loss.
- Li, Z., Muller, J. P., Cross, P., & Fielding, E. J. (2005). Interferometric synthetic aperture radar (InSAR) atmospheric correction: GPS, Moderate Resolution Imaging Spectroradiometer (MODIS), and InSAR integration. *Journal of Geophysical Research: Solid Earth (1978–2012)*, 110(B3).
- Li, Z., Bao, Z., & Suo, Z. (2007). A joint image coregistration, phase noise suppression, and phase unwrapping method based on subspace projection for multibaseline InSAR systems. *Geoscience and Remote Sensing, IEEE Transactions on*, 45(3), 584-591.
- Li, Z., Bao, Z., Li, H., & Liao, G. (2006). Image autocoregistration and InSAR interferogram estimation using joint subspace projection. *Geoscience and Remote Sensing, IEEE Transactions on*, 44(2), 288-297.
- Lin, C.H. (2005) Seismicity increase after the construction of the world's tallest building: An active blind fault beneath the Taipei 101 *Geophysical Research Letters*, 32 (2005), p. L22313
- Liu, G., Ding, X., Y. Chen, Z. Li, Z. Li (2001) Ground settlement of Chek Lap Kok Airport, Hong Kong, detected by satellite synthetic aperture radar interferometry *Chinese Science Bulletin*, 46 (21), pp. 1778–1782
- Liu, G., Luo, X., Chen, Q., Huang, D., & Ding, X. (2008). Detecting land subsidence in Shanghai by PS-networking SAR interferometry. *Sensors*, 8(8), 4725-4741.

- Liu, L., Zhang, T., & Wahr, J. (2010). InSAR measurements of surface deformation over permafrost on the North Slope of Alaska. *Journal of Geophysical Research: Earth Surface (2003–2012)*, 115(F3).
- Liu, L., Jafarov, E. E., Schaefer, K. M., Jones, B. M., Zebker, H. A., Williams, C. A., ... & Zhang, T. (2014). InSAR detects increase in surface subsidence caused by an Arctic tundra fire. *Geophysical Research Letters*, 41(11), 3906-3913.
- Li, F. K., & Goldstein, R. M. (1990). Studies of multibaseline spaceborne interferometric synthetic aperture radars. *Geoscience and Remote Sensing, IEEE Transactions on*, 28(1), 88-97.
- Li, Z., Muller, J. P., Cross, P., & Fielding, E. J. (2005). Interferometric synthetic aperture radar (InSAR) atmospheric correction: GPS, Moderate Resolution Imaging Spectroradiometer (MODIS), and InSAR integration. *Journal of Geophysical Research: Solid Earth*, 110(B3).
- Li, Z., Bao, Z., Li, H., & Liao, G. (2006). Image autocoregistration and InSAR interferogram estimation using joint subspace projection. *IEEE Transactions on Geoscience and Remote Sensing*, 44(2), 288-297.
- Li, Z., Bao, Z., & Suo, Z. (2007). A joint image coregistration, phase noise suppression, and phase unwrapping method based on subspace projection for multibaseline InSAR systems. *IEEE transactions on geoscience and remote sensing*, 45(3), 584-591.
- Li, Z., Elliott, J. R., Feng, W., Jackson, J. A., Parsons, B. E., & Walters, R. J. (2011). The 2010 Mw 6.8 Yushu (Qinghai, China) earthquake: constraints provided by InSAR and body wave seismology. *Journal of Geophysical Research: Solid Earth*, 116(B10).
- Li, Z. W., Xu, W. B., Feng, G. C., Hu, J., Wang, C. C., Ding, X. L., & Zhu, J. J. (2012). Correcting atmospheric effects on InSAR with MERIS water vapour data and elevation-dependent interpolation model. *Geophysical journal international*, 189(2), 898-910.

- Liu, Z., Jung, H. S., & Lu, Z. (2014). Joint correction of ionosphere noise and orbital error in L-band SAR interferometry of interseismic deformation in southern California. *Geoscience and Remote Sensing, IEEE Transactions on*, 52(6), 3421-3427.
- Liang, C., Zeng, Q., Jia, J., & Jiao, J. (2013). ScanSAR interferometric processing using existing standard InSAR software for measuring large scale land deformation. *Computers & Geosciences*, 51, 439-448.
- Loffeld, O., Nies, H., Knedlik, S., & Wang, Y. (2008). Phase unwrapping for SAR interferometry—A data fusion approach by Kalman filtering. *Geoscience and Remote Sensing, IEEE Transactions on*, 46(1), 47-58.
- Lopes, A., Nezry, E., Touzi, R., & Laur, H. (1993). Structure detection and statistical adaptive speckle filtering in SAR images. *International Journal of Remote Sensing*, 14(9), 1735-1758.
- López-Quiroz, Penélope, et al. "Time series analysis of Mexico City subsidence constrained by radar interferometry." *Journal of Applied Geophysics* 69.1 (2009): 1-15.
- Lu, Z., & Danskin, W. R. (2001). InSAR analysis of natural recharge to define structure of a ground-water basin, San Bernardino, California. *Geophysical Research Letters*, 28(13), 2661-2664.
- Lu, D., Batistella, M., Moran, E., 2007. Land-cover classification in the Brazilian Amazon with the integration of Landsat ETM+ and RADARSAT data. *International Journal of Remote Sensing*, 28(4): pp. 5447-5459.
- Lu, Z. Kwoun, O., & Rykhus, R. (2007). Interferometric synthetic aperture radar (InSAR): its past, present and future. *Photogrammetric engineering and remote sensing*, 73(3), 217.
- Lu, Zhong, and O-I. Kwoun. "Radarsat-1 and ERS InSAR analysis over southeastern coastal Louisiana: Implications for mapping water-level changes beneath swamp forests." *Geoscience and Remote Sensing, IEEE Transactions on* 46.8 (2008): 2167-2184

- Luo, X. J., Huang, D. F., & Liu, G. X. (2006). Phase decomposition of interferometric synthetic aperture radar and relevant application in DEM formation and research on earthquake deformation field. *Northwestern Seismological Journal*, 28(3), 204-209.
- Lyons, S., and D. Sandwell (2003), Fault creep along the southern San Andreas from interferometric synthetic aperture radar, permanent scatterers, and stacking. *J. Geophys. Res.*, 108(B1), 2047
- Malinverni, E. S., Sandwell, D. T., Tasseti, A. N., & Cappelletti, L. (2014). InSAR decorrelation to assess and prevent volcanic risk. *European Journal of Remote Sensing*, 47, 537-556.
- Manaker, D.M., Michael, A.J., and Burgmann, R., (2005), Subsurface structure and mechanics of the Calaveras Hayward fault stepover from three-dimensional vp and seismicity, San Francisco Bay region, California: Bulletin of the Seismological Society of America, v. 95, p. 446–470
- Manap, M. A., Sulaiman, W. N. A., Ramli, M. F., Pradhan, B., & Surip, N. (2013). A knowledge-driven GIS modeling technique for groundwater potential mapping at the Upper Langat Basin, Malaysia. *Arabian Journal of Geosciences*, 6(5), 1621-1637.
- Manunta, M. (2009). New Advances in Multi-Temporal Differential SAR Interferometry for Full Resolution Data Analysis.
- Martire, D., Iglesias, R., Monells, D., Centolanza, G., Sica, S., Ramondini, M., ... & Calcaterra, D. (2014). Comparison between Differential SAR interferometry and ground measurements data in the displacement monitoring of the earth-dam of Conza della Campania (Italy). *Remote Sensing of Environment*, 148, 58-69.
- Martire, D., A. Iodice, M. Ramondini, G. Ruello, D. Calcaterra (2011) Combined observations of surface displacements using Differential Interferometry SAR (DInSAR) and traditional monitoring techniques Proc. 8th Intern. Symp. on Field Measurements in GeoMechanics, Berlin, Germany, September 12–16, 2011 (13 pp.)

- MarwaChendeb El Rai and Elisabeth Simonetto (2004) à la ville de Paris, A. Mesure des déformations du sol par la méthode des réflecteurs permanents StaMPS.
- Marques, P. A., & Bioucas Dias, J. M. (2007). Moving targets processing in SAR spatial domain. *Aerospace and Electronic Systems, IEEE Transactions on*, 43(3), 864-874.
- Massonnet, D., & Feigl, K. L. (1998). Radar interferometry and its application to changes in the Earth's surface. *Reviews of geophysics*, 36(4), 441-500.
- Massonnet, D., Briole, P., & Arnaud, A. (1995). Deflation of Mount Etna monitored by spaceborne radar interferometry.
- Massonnet, D., Rossi, M., Carmona, C., Adragna, F., Peltzer, G., Feigl, K., & Rabaute, T. (1993). The displacement field of the Landers earthquake mapped by radar interferometry. *Nature*, 364(6433), 138-142.
- Meisina, C., Zucca, F., Notti, D., Colombo, A., Cucchi, A., Savio, G., ... & Bianchi, M. (2008). Geological interpretation of PSInSAR data at regional scale. *Sensors*, 8(11), 7469-7492.
- Meyer, B., Armijo, R., Massonnet, D., De Chabalier, J. B., Delacourt, C., Ruegg, J. C., ... & Papanastassiou, D. (1996). The 1995 Grevena (Northern Greece) earthquake: fault model constrained with tectonic observations and SAR interferometry. *Geophysical research letters*, 23(19), 2677-2680.
- Meyer, F., Bamler, R., Jakowski, N., and Fritz, T. (2006). The potential of low-frequency SAR systems for mapping ionospheric TEC distributions. *Geoscience and Remote Sensing Letters, IEEE*, 3(4), 560-564.
- Mikkelsen, P. E. (1996). Field instrumentation. *AK Turner and RL Schuster, op. cit*, 278-314.
- Mirek, K., & Mirek, J. (2011). Correlation between ground subsidence and induced mining seismicity, Upper Silesia Coal Basin case study. *Polish Journal of Environmental Studies*, 20(4A), 253-257.

- Moholdt, G., & Kääb, A. (2012). A new DEM of the Austfonna ice cap by combining differential SAR interferometry with ICESat laser altimetry. *Polar Research*, 31.
- Mora, maps from a reduced set of interferometric SAR images. *Geoscience and Remote Sensing, IEEE Transactions on*, 41(10), 2243-2253.
- Motagh, M., Djamour, Y., Walter, T. R., Wetzell, H. U., Zschau, J., and Arabi, S. (2007). Land subsidence in Mashhad Valley, northeast Iran: results from InSAR, levelling and GPS. *Geophysical Journal International*, 168(2), 518-526.
- Muhamad, N., Lim, C. S., Reza, M. I. H., & Pereira, J. J. (2015, August). Urban hazards management: A case study of Langat river basin, Peninsular Malaysia. In *2015 International Conference on Space Science and Communication (IconSpace)* (pp. 438-443). IEEE.
- Nico, G., Pappalepore, M., Pasquariello, G., Refice, A., & Samarelli, S. (2000). Comparison of SAR amplitude vs. coherence flood detection methods-a GIS application. *International Journal of Remote Sensing*, 21(8), 1619-1631.
- Nikolakopoulos, K. G., Kamaratakis, E. K., & Chrysoulakis, N. (2006). SRTM vs ASTER elevation products. Comparison for two regions in Crete, Greece. *International Journal of remote sensing*, 27(21), 4819-4838.
- Noferini, L., Pieraccini, M., Mecatti, D., Luzi, G., Atzeni, C., Tamburini, A., and Broccolato, M. (2005). Permanent scatterers analysis for atmospheric correction in ground-based SAR interferometry. *Geoscience and Remote Sensing, IEEE Transactions on*, 43(7), 1459-1471.
- Ortega-Guerrero, A., Rudolph, D. L., and Cherry, J. A. (1999). Analysis of long-term land subsidence near Mexico City: Field investigations and predictive modeling. *Water Resources Research*, 35(11), 3327-3341.
- Osmanoğlu, Batuhan, et al. "Mexico City subsidence observed with persistent scatterer InSAR." *International Journal of Applied Earth Observation and Geoinformation* 13.1 (2011): 1-12.

- Ouchi, K., Tamaki, S., Yaguchi, H., & Iehara, M. (2004). Ship detection based on coherence images derived from cross correlation of multilook SAR images. *Geoscience and Remote Sensing Letters, IEEE*, 1(3), 184-187.
- Parizzi, Alessandro, and Ramon Brcic. "Adaptive InSAR stack multilooking exploiting amplitude statistics: A comparison between different techniques and practical results." *Geoscience and Remote Sensing Letters, IEEE* 8.3 (2011): 441-445.
- Peltzer, G., and P. A. Rosen, (1995), Surface displacement of the 17 May 1993 Eureka Valley, California, earthquake observed by SAR interferometry, *Science*, 268, 1333-1336,.
- Pepe, A., Sansosti, E., Berardino, P., & Lanari, R. (2005). On the generation of ERS/ENVISAT DInSAR time-series via the SBAS technique. *Geoscience and Remote Sensing Letters, IEEE*, 2(3), 265-269.
- Perissin, D., Pichelli, E., Ferretti, R., Rocca, F., & Pierdicca, N. (2009). The MM5 numerical model to correct PSInSAR atmospheric phase screen. *In Proceedings of FRINGE*.
- Perissin, D., & Wang, T. (2011). Time-series InSAR applications over urban areas in China. *Selected Topics in Applied Earth Observations and Remote Sensing, IEEE Journal of*, 4(1), 92-100
- Perissin, D., and Rocca, F. (2006). High-accuracy urban DEM using permanent scatterers. *Geoscience and Remote Sensing, IEEE Transactions on*, 44(11), 3338-3347.
- Perski, Z. (1998). Applicability of ERS-1 and ERS-2 InSAR for land subsidence monitoring in the Silesian coal mining region, Poland. *International Archives of Photogrammetry and Remote Sensing*, 32, 555-558.
- Perski, Z., Hanssen, R., Wojcik, A., & Wojciechowski, T. (2009). InSAR analyses of terrain deformation near the Wieliczka Salt Mine, Poland. *Engineering Geology*, 106(1), 58-67.

- Piątkowska, A., Graniczny, M., Surafa, M., & Perski, Z. (2011, September). Application of SAR interferometric methods to identify the mobility of the area above salt diapir in Inowrocław City, Kujawy region (Poland) Abstract. In *FRINGE 2011 Workshop* (pp. 19-23).
- Pourebrahim, S., Hadipour, M., & Mokhtar, M. B. (2011). Integration of spatial suitability analysis for land use planning in coastal areas; case of Kuala Langat District, Selangor, Malaysia. *Landscape and Urban Planning*, 101(1), 84-97.
- Pourebrahim, S., Hadipour, M., & Mokhtar, M. B. (2015). Impact assessment of rapid development on land use changes in coastal areas; case of Kuala Langat district, Malaysia. *Environment, Development and Sustainability*, 17(5), 1003-1016.
- Prati, C., Ferretti, A., & Perissin, D. (2010). Recent advances on surface ground deformation measurement by means of repeated space-borne SAR observations. *Journal of Geodynamics*, 49(3), 161-170.
- Puysségur, B., Michel, R., and Avouac, J.-P. (2007), Tropospheric phase delay in interferometric synthetic aperture radar estimated from meteorological model and multispectral imagery, *J. Geophys. Res.*, 112, B05419
- Perissin, D., & Rocca, F. (2006). High-accuracy urban DEM using permanent scatterers. *IEEE Transactions on Geoscience and Remote Sensing*, 44(11), 3338-3347.
- Perissin, D., Prati, C., Rocca, F., & Wang, T. (2009, May). PSInSAR analysis over the Three Gorges Dam and urban areas in China. In *2009 Joint Urban Remote Sensing Event* (pp. 1-5). IEEE.
- Perissin, D., Pichelli, E., Ferretti, R., Rocca, F., & Pierdicca, N. (2009). The MM5 numerical model to correct PSInSAR atmospheric phase screen. In *Proceedings of FRINGE*.
- Perissin, D., & Wang, T. (2011). Time-series InSAR applications over urban areas in China. *IEEE journal of selected topics in applied earth observations and remote sensing*, 4(1), 92-100.

- Qiao, X., Yang, S., Du, R., Ge, L., & Wang, Q. (2011). Coseismic Slip from the 6 October 2008, Mw 6.3 Damxung Earthquake, Tibetan Plateau, Constrained by InSAR Observations. *Pure and applied geophysics*, 168(10), 1749-1758.
- Raymond, D., & Rudant, J. P. (1997). ERS-SAR interferometry: Potential and limits for mining subsidence detection. *European Space Agency-Publications-Esa Sp*, 414, 541-544.
- Reigber, C., Xia, Y., Kaufmann, H., Massmann, F. H., Timmen, L., Bodechtel, J., & Frei, M. (1997, March). Impact of precise orbits on SAR interferometry. In *ERS SAR Interferometry* (Vol. 406, p. 223).
- Remy, D., Bonvalot, S., Briole, P., Murakami, M. (2003), Accurate measurements of tropospheric effects in volcanic areas from SAR interferometry data: application to Sakurajima volcano (Japan) *Earth Planet. Sci. Lett.*, 213, pp. 299–310
- Riddick S.N., D.A. Schmidt, N.I. Deligne, 2012,,An analysis of terrain properties and the location of surface scatterers from persistent scatterer interferometry, *ISPRS Journal of Photogrammetry and Remote Sensing* 73, 50-57
- Rigo, A., & Massonnet, D. (1999). Investigating the 1996 Pyrenean earthquake (France) with SAR interferograms heavily distorted by atmosphere. *Geophysical Research Letters*, 26(21), 3217-3220.
- Robertson, E. A. M., Biggs, J., Cashman, K. V., Floyd, M. A., & Vye-Brown, C. (2015). Influence of regional tectonics and pre-existing structures on the formation of elliptical calderas in the Kenyan Rift. *Geological Society, London, Special Publications*, 420, SP420-12.
- Rodriguez, E., and J. M. Martin. "Theory and design of interferometric synthetic aperture radars." *Radar and Signal Processing, IEE Proceedings F*. Vol. 139. No. 2. IET, 1992.
- Rosen, P. A., Hensley, S., Joughin, I. R., Li, F. K., Madsen, S. N., Rodriguez, E., and Goldstein, R. M. (2000). Synthetic aperture radar interferometry. *Proceedings of the IEEE*, 88(3), 333-382.

- Rudolf, H., Leva, D., Tarchi, D., & Sieber, A. J. (1999). A mobile and versatile SAR system. In *Geoscience and Remote Sensing Symposium, 1999. IGARSS'99 Proceedings. IEEE 1999 International (Vol. 1, pp. 592-594)*. IEEE
- Rufino, G., Moccia, A., & Esposito, S. (1998). DEM generation by means of ERS tandem data. *Geoscience and Remote Sensing, IEEE Transactions on*, 36(6), 1905-1912.
- Saastamoinen, J., 1972. Atmospheric correction for the troposphere and stratosphere in radio ranging of satellites. In: *The Use of Artificial Satellites for Geodesy, Geophysical Monograph Series, vol. 15*. AGU, Washington, DC, pp. 247–251.
- Saffuan, R., Ariffin, J., & Amin, Z. (2013). Green technology design approach for liveable park of Tasik Biru Kundang, Malaysia. *Asian Journal of Environment-Behaviour Studies*, 4(11), 39-48.
- Sahu, P. , and Sikdar, P. K. (2011). Threat of land subsidence in and around Kolkata City and East Kolkata Wetlands, West Bengal, India. *Journal of earth system science*, 120(3), 435-446.
- Samsonov, S., Tiampo, K., González, P. J., Manville, V., and Jolly, G. (2010). Ground deformation occurring in the city of Auckland, New Zealand, and observed by Envisat interferometric synthetic aperture radar during 2003–2007. *Journal of Geophysical Research: Solid Earth (1978–2012)*, 115(B8).
- Sandwell, D. T., and Price, E. J. (1998). Phase gradient approach to stacking interferograms. *Journal of Geophysical Research: Solid Earth (1978–2012)*, 103(B12), 30183-30204.
- Sandwell, D. T., Sichoix, L., Agnew, D., Bock, Y., & Minster, J. B. (2000). Near real-time radar interferometry of the Mw 7.1 Hector Mine Earthquake. *Geophysical Research Letters*, 27(19), 3101-3104.
- Sandwell, D. T., Myer, D., Mellors, R., Shimada, M., Brooks, B., & Foster, J. (2008). Accuracy and resolution of ALOS interferometry: Vector deformation maps of the Father's Day intrusion at Kilauea. *IEEE Transactions on Geoscience and Remote Sensing*, 46(11), 3524-3534.

- Sansosti, E Berardino, P., Manunta, M., Serafino, F., & Fornaro, G. (2006). Geometrical SAR image registration. *Geoscience and Remote Sensing, IEEE Transactions on*, 44(10), 2861-2870.
- Schreier, G., Kosmann, D., & Roth, A. (1990). Design aspects and implementation of a system for geocoding satellite SAR-images. *ISPRS journal of Photogrammetry and Remote Sensing*, 45(1), 1-16.
- Shanker, A. P., & Zebker, H. (2010). Edgelist phase unwrapping algorithm for time series InSAR analysis. *JOSA A*, 27(3), 605-612.
- Shimada, M., & Hirose, H. (2000). Slope corrections to normalized RCS using SAR interferometry. *Geoscience and Remote Sensing, IEEE Transactions on*, 38(3), 1479-1484.
- Shirzaei, M., and Walter, T. R. (2011). Estimating the effect of satellite orbital error using wavelet-based robust regression applied to InSAR deformation data. *Geoscience and Remote Sensing, IEEE Transactions on*, 49(11), 4600-4605.
- Sousa, J J., Ruiz, A. M., Hanssen, R. F., Bastos, L., Gil, A. J., Galindo-Zaldívar, J., and de Galdeano, C. S. (2010). PS-InSAR processing methodologies in the detection of field surface deformation—Study of the Granada basin (Central Betic Cordilleras, southern Spain). *Journal of Geodynamics*, 49(3), 181-189.
- Sousa, Joaquim J., et al. "Persistent scatterer InSAR: a comparison of methodologies based on a model of temporal deformation vs. spatial correlation selection criteria." *Remote Sensing of Environment* 115.10 (2011): 2652-2663.
- Sousa, Joaquim J., et al. "PS-InSAR processing methodologies in the detection of field surface deformation—Study of the Granada basin (Central Betic Cordilleras, southern Spain)." *Journal of Geodynamics* 49.3 (2010): 181-189.
- Sousa, J. J., Bastos, L. C., Ruiz, A. M., Hooper, A. J., & Hanssen, R. (2012, January). Detection Of Ground Deformation In The Oporto Metropolitan Area With Multi-Temporal Interferometry (MTI). In *Fringe 2011*(Vol. 697, pp. 92-9092).

- Sowter, A. (2003). The derivation of phase integer ambiguity from single InSAR pairs: implications for differential interferometry. In *Proceedings of the 11th FIG Symposium on Deformation Measurements, Santorini, Greece* (pp. 149-156).
- Stek, P. E. (2008). Urban groundwater extraction in Kuala Lumpur, Malaysia.
- Stilla, U., Soergel, U., & Thoennessen, U. (2003). Potential and limits of InSAR data for building reconstruction in built-up areas. *ISPRS Journal of Photogrammetry and Remote Sensing*, 58(1), 113-123.
- Strozzi, T., U. Wegmuller, et al, 2003. Validation of the X-SAR SRTM DEM for ERS and JERS SAR geocoding and 2-pass differential interferometry in alpine regions. Igarss 2003: Ieee International Geoscience and Remote Sensing Symposium, Vols I - Vii, Proceedings - Learning from Earth's Shapes and Sizes. New York, IEEE, pp.109-111.
- Stumpf, A., Malet, J. P., Kerle, N., Niethammer, U., & Rothmund, S. (2013). Image-based mapping of surface fissures for the investigation of landslide dynamics. *Geomorphology*, 186, 12-27.
- Sun, Q., Zhang, L., Ding, X. L., Hu, J., Li, Z. W., & Zhu, J. J. (2015). Slope deformation prior to Zhouqu, China landslide from InSAR time series analysis. *Remote Sensing of Environment*, 156, 45-57.
- Tamburini, A., Falorni, G., Novali, F., Fumagalli, A., & Ferretti, A. (2010, March). Advances in reservoir monitoring using satellite radar sensors. In *Geophysical Research Abstracts* (pp. 2010-10689).
- Tan, M. P., Jamsari, A. F. J., & Azizah, M. N. S. (2012). Phylogeographic pattern of the striped snakehead, *Channa striata* in Sundaland: ancient river connectivity, geographical and anthropogenic signatures. *PloS one*, 7(12), e52089.
- Tantianuparp, P., Shi, X., Zhang, L., Balz, T., & Liao, M. (2013). Characterization of landslide deformations in three gorges area using multiple InSAR data stacks. *Remote Sensing*, 5(6), 2704-2719.

- Teatini, P., Ferronato, M., Gambolati, G., and Gonella, M. (2006). Groundwater pumping and land subsidence in the Emilia-Romagna coastland, Italy: Modeling the past occurrence and the future trend. *Water Resources Research*, 42(1).
- Teh, T. C., Palmer, A. C., & Damgaard, J. S. (2003). Experimental study of marine pipelines on unstable and liquefied seabed. *Coastal Engineering*, 50(1), 1-17.
- The Star (2014) retrieved on 13 July 2016 from <http://www.thestar.com.my/news/nation/2014/05/23/klia2-sinking/>
- Thiel, K-H., Wu, X.-Q. and Hartl, P., (1997). ERS-tandem-interferometric observation of volcano activities in Iceland. The 3rd ERS SYMPOSIUM, Florence, 17 - 21 March 1997.
- Tiwari, A., Dwivedi, R., Narayan, A. B., Dikshit, O., & Singh, A. K. (2014). Efficacy of StaMPS technique for monitoring surface deformation in L'Aquila, Italy. *The International Archives of Photogrammetry, Remote Sensing and Spatial Information Sciences*, 40(8), 141.
- Tong, X., Sandwell, D. T., & Fialko, Y. (2010). Coseismic slip model of the 2008 Wenchuan earthquake derived from joint inversion of interferometric synthetic aperture radar, GPS, and field data. *Journal of Geophysical Research: Solid Earth*, 115(B4).
- Touzi, R., Lopes, A., Bruniquel, J., & Vachon, P. W. (1999). Coherence estimation for SAR imagery. *Geoscience and Remote Sensing, IEEE Transactions on*, 37(1), 135-149.
- Usai, Stefania. "The use of man-made features for long time scale insar." *Geoscience and Remote Sensing, 1997. IGARSS'97. Remote Sensing-A Scientific Vision for Sustainable Development., 1997 IEEE International*. Vol. 4. IEEE, 1997.
- Usai, Stefania, and Ramon Hanssen. "Long time scale INSAR by means of high coherence features." *EUROPEAN SPACE AGENCY-PUBLICATIONS-ESA SP 414 (1997)*: 225-228.

- Vallone, P., Giammarinaro, M. S., Crosetto, M., Agudo, M., & Biescas, E. (2008). Ground motion phenomena in Caltanissetta (Italy) investigated by InSAR and geological data integration. *Engineering geology*, 98(3), 144-155.
- Van Westen, C. J., & Soeters, R. (2000). Remote sensing and geographic information systems for natural disaster management. Roy, P.; van Westen, CJ and P. Champati Ray (Eds.): *Natural Disasters and their mitigation. A Remote Sensing and GIS Perspective. Indian Institute of Remote Sensing. National Remote Sensing Agency, India*, 31-76.
- Velez, M. L., Euillades, P., Caselli, A., Blanco, M., & Díaz, J. M. (2011). Deformation of Copahue volcano: inversion of InSAR data using a genetic algorithm. *Journal of Volcanology and Geothermal Research*, 202(1), 117-126.
- Ventisette, D. C., Ciampalini, A., Manunta, M., Calò, F., Paglia, L., Ardizzone, F., ... & Garcia, I. (2013). Exploitation of large archives of ERS and ENVISAT C-band SAR data to characterize ground deformations. *Remote Sensing*, 5(8), 3896-3917.
- Villano, M., & Krieger, G. (2012). Impact of azimuth ambiguities on interferometric performance. *IEEE Geoscience and Remote Sensing Letters*, 9(5), 896-900
- Vilardo, G., et al. "InSAR Permanent Scatterer analysis reveals fault re-activation during inflation and deflation episodes at Campi Flegrei caldera." *Remote Sensing of Environment* 114.10 (2010): 2373-2383.
- Wadge, G., et al. (2002), Atmospheric models, GPS and InSAR measurements of the tropospheric water vapour field over Mount Etna, *Geophys. Res. Lett.*, 29(19), 1905
- Wallace, L. M., Barnes, P., Beavan, J., Van Dissen, R., Litchfield, N., Mountjoy, J., ... & Pondard, N. (2012). The kinematics of a transition from subduction to strike-slip: An example from the central New Zealand plate boundary. *Journal of Geophysical Research: Solid Earth*, 117(B2).
- Wang, H., and Wright, T. J. (2012). Satellite geodetic imaging reveals internal deformation of western Tibet. *Geophysical Research Letters*, 39(7).

- Wang, H., Wright, T. J., & Biggs, J. (2009). Interseismic slip rate of the northwestern Xianshuihe fault from InSAR data. *Geophysical Research Letters*, 36(3).
- Webley, P. W. (2003). *Atmospheric water vapour correction to InSAR surface motion measurements on mountains: Case Study on Mount Etna* (Doctoral dissertation, University of Reading).
- Webley, P. W., Bingley, R. M., Dodson, A. H., Wadge, G., Waugh, S. J., and James, I. N. (2002). Atmospheric water vapour correction to InSAR surface motion measurements on mountains: results from a dense GPS network on Mount Etna. *Physics and Chemistry of the Earth, Parts A/B/C*, 27(4), 363-370.
- Wegmuller, U., Werner, C., Strozzi, T., and Wiesmann, A. (2006). Ionospheric electron concentration effects on SAR and INSAR. In *Geoscience and Remote Sensing Symposium, 2006. IGARSS 2006. IEEE International Conference on* (pp. 3731-3734).
- Werner, C., T. Strozzi, et al, 2002. SAR geocoding and multi-sensor image registration. *Igarss 2002: Ieee International Geoscience and Remote Sensing Symposium and 24th Canadian Symposium on Remote Sensing*,
- Werner, C., U. Wegmüller, T. Strozzi, and A. Wiesmann (2006), Interferometric point target analysis for deformation mapping, paper presented at International Geoscience and Remote Sensing Symposium, Toulouse, France. Kamps, B. M.. *Radar Interferometry*. Springer.
- Williams, S., Bock, Y., & Fang, P. (1998). Integrated satellite interferometry: Tropospheric noise, GPS estimates and implications for interferometric synthetic aperture radar products. *Journal of Geophysical Research: Solid Earth (1978–2012)*, 103(B11), 27051-27067.
- Wilson, S. D., and Mikkelsen, P. E. (1978). Field instrumentation. *Transportation Research Board Special Report*, (176).
- Woodhouse I.H., Predicting backscatter-biomass and height-biomass trends using a macroecology model, *IEEE Transactions on Geoscience and Remote Sensing*, 44 (2006), pp. 871–877

- Worawattanamateekul, J., Hoffmann, J., Adam, N., & Kampes, B. (2003, December). Urban deformation monitoring in BANGKOK metropolitan (Thailand) using permanent scatterer and differential interferometry techniques. In *Proceedings of FRINGE* (pp. 1-5).
- Xiao, R., & He, X. (2013). GPS and InSAR Time Series Analysis: Deformation Monitoring Application in a Hydraulic Engineering Resettlement Zone, Southwest China. *Mathematical Problems in Engineering*, 2013.
- Xing, M., Jiang, X., Wu, R., Zhou, F., & Bao, Z. (2009). Motion compensation for UAV SAR based on raw radar data. *Geoscience and Remote Sensing, IEEE Transactions on*, 47(8), 2870-2883
- Xuedong, Z., Daqing, G., Weiyu, M., Ling, Z., Yan, W., & Xiaofang, G. (2011, July). Study the land subsidence along JingHu highway (Beijing-Hebei) using PS-InSAR technique. In *Geoscience and Remote Sensing Symposium (IGARSS), 2011 IEEE International* (pp. 1608-1611). IEEE.
- Yoo, C., & Lee, D. (2008). Deep excavation-induced ground surface movement characteristics—A numerical investigation. *Computers and Geotechnics*, 35(2), 231-252
- Yun, S. H., Zebker, H., Segall, P., Hooper, A., & Poland, M. (2007). Interferogram formation in the presence of complex and large deformation. *Geophysical Research Letters*, 34(12).
- Zebker, H. A., and J. Villasenor (1992), Decorrelation in interferometric radar echoes, *IEEE Trans. Geosci. Remote Sens.*, **30**,950–959.
- Zebker, H. A., Rosen, P. A., & Hensley, S. (1997). Atmospheric effects in interferometric synthetic aperture radar surface deformation and topographic maps. *Journal of Geophysical Research: Solid Earth*, 102(B4), 7547-7563.
- Zebker, H., Shankar, P., & Hooper, A. (2007, April). InSAR remote sensing over decorrelating terrains: persistent scattering methods. In *2007 IEEE Radar Conference* (pp. 717-722). IEEE.

- Zhao, C. Y., Zhang, Q., Ding, X. L., Lu, Z., Yang, C. S., and Qi, X. M. (2009). Monitoring of land subsidence and ground fissures in Xian, China 2005–2006: mapped by SAR interferometry. *Environmental geology*, 58(7), 1533–1540.
- Zhang, Yanjie, and Véronique Prinnet. "InSAR coherence estimation." *IGARSS*. 2004.
- Zhou Yueqin, Zheng Zhaobao, Li Deren et al., 1998. SAR stereo positioning principle and accuracy analysis. *Journal of Remote Sensing*, 2(4): 245–250. (in Chinese)
- Zhou X, Chang N-B, Li S. Applications of SAR Interferometry in Earth and Environmental Science Research. *Sensors*. 2009; 9(3):1876-1912.
- Zhao, C., Lu, Z., Zhang, Q., Yang, C., & Zhu, W. (2014). Mining collapse monitoring with SAR imagery data: a case study of Datong mine, China. *Journal of Applied Remote Sensing*, 8(1), 083574-083574.
- Žibret, G., Komac, M., & Jemec, M. (2012). PSInSAR displacements related to soil creep and rainfall intensities in the Alpine foreland of western Slovenia. *Geomorphology*, 175, 107-114.
- Zizzi, Stephen. (2013) *Real estate disclosure reporting method U.S*, Patent Application 14/104,682.